RESEARCH INVESTIGATION OF LASER LINE PROFILES (PICOSECOND LASER PULSES)

REPORT G920479-8
SECOND ANNUAL REPORT

PERIOD COVERED: 1 AUGUST 1967 TO 31 JULY 1968

PREPARED UNDER CONTRACT N00014-66-C0344

ARPA ORDER NO. 306, PROJECT COST CODE NO. 6E30K21

United Aircraft Research Laboratories

UNITED AIRCRAFT CORPORATION

EAST HARTFORD, CONNECTICUT

UNITED AIRCRAFT CORPORATION
RESEARCH LABORATORIES
East Hartford, Connecticut

G-920479-8
Annual Report Under
Contract N00014-66-C0344
1 August 1967
through
31 July 1968

Project Title: RESEARCH INVESTIGATION OF LASER LINE PROFILES
Name of Contractor: United Aircraft Corporation Research Laboratories
Project Code No. 6E30K21
ARPA Order No. 306

This research is part of Project DEFENDER under the joint sponsorship of the Advanced Research Projects Agency, the Office of Naval Research, and the Department of Defense.

Reported By:

M. J. Brienza
Chief, Applied Laser Technology

A. J. DeMaria
Senior Principal Scientist
Quantum Physics Laboratory

W. H. Glenn, Jr.
Principal Scientist,
Quantum Physics

G. L. Lamb, Jr.
Senior Theoretical Physicist

M. E. Mack
Senior Research Scientist

E. B. Treacy
Senior Research Scientist

Approved By:

A. J. DeMaria
Senior Principal Scientist
Quantum Physics Laboratory

Date: August 28, 1968

Report G-920479-8

Annual Report Under Contract N00014-66-C0344
for the Period 1 August 1967 through 31 July 1968

RESEARCH INVESTIGATION OF LASER LINE PROFILES
(Picosecond Laser Pulses)

ARPA Order No. 306, Project Code No. 6E30K21

TABLE OF CONTENTS

TABLE OF CONTENTS (Cont'd)

Report G-920479-8

Annual Report under Contract N00014-66-C0344
for the Period 1 August 1967 to 31 July 1968

Research Investigation of Laser Line Profiles

(Picosecond Laser Pulses)

ARPA Order No. 306, Project Code No. 6E30K21

SUMMARY

This report presents a summary of the research performed by the United Aircraft Research Laboratories during the twelve-month interval from 1 August 1967 to 31 July 1968 on problems concerned with advancing the state of the art of ultrashort laser pulse technology. The effort has resulted in the following acccmplishments:

(a) Analysis of the Propagation of Ultrashort Optical Pulses. A description is given of a theoretical model which accounts for certain novel effects that take place when extremely short pulses of coherent light interact with matter. It is shown that the interaction of an assembly of two-level systems with a light pulse having a duration that is short compared to all relaxation times of these systems can be described in terms of a single nonlinear partial differential equation. The equation is one which also occurs in differential geometry. Techniques available for obtaining particular solutions of this equation may be employed to derive analytical expressions which describe the observed breakup of short pulses as well as the self-induced transparency effect. Analytical solutions describing the propagation of 2π and 4π pulses have been derived and could be generalized to describe the behavior of 2π pulses.

(b) Measurement of Nanosecond Fluorescence Decay Times. This accomplishment has demonstrated how ultrashort laser pulses of high peak power may be used to measure nanosecond fluorescent lifetimes. The techniques can be extended to the measurement of subnanosecond decay times.

(c) Light Amplification in Saturable Absorbers (LAISA) with Picosecond Pulses. It has been found that an absorber, driven into saturation by an intense light pulse from a mode-locked ruby laser, can amplify a weaker light pulse simultaneously incident upon the medium. Energy gains as high as 20 times have been observed in a 1 cm path length in the saturable absorber solution. A theory giving qualitative agreement with the experimental results has been developed. The effect has an important bearing on the subject of mode-locking with saturable absorbers.

(d) Adiabatic Inversion of Quantum States. A theoretical investigation of the interaction of an intense, frequency-swept pulse of light (i.e., an optical chirp) with matter has been conducted. The first interesting result to come out of the investigation was the adiabatic inversion of populations between a pair of levels when the frequency of the pulse is swept through their resonant frequency. The second result was the dependence of the phase of the induced polarization on the direction of the sweep. An experiment to attempt to observe these effects is in progress. In connection with this experiment a 60 MHz frequency swept, Q-switched CO_2 laser has been developed. This should also have application to problems in optical ranging and signal processing.

(e) Optical Rectification of Mode-Locked Laser Pulses at Microwave Frequencies. This accomplishment opens up the possibility of generating millimeter or submillimeter waves with ultrashort optical pulses and obtaining a detector for picosecond pulses because of the broad band response of the optical rectification effect. The detection of optical rectification at approximately 10 GHz has eliminated spurious signals from pyroelectric and acoustic effects, therefore simplifying the detection of this effect. The use of simultaneously Q-switched and mode-locked pulses enables the use of the high sensitivity characteristics of radio receivers in many experiments where signal sensitivity may be a problem.

(f) Mode-locking of Organic Dye Lasers. A laser-pumped organic dye laser has been developed and has resulted in the production of subnanosecond (possibly picosecond) pulses at the dye laser wavelength. Further work in this area should make available picosecond optical pulses throughout the visible portion of the spectrum. The availability of ultrashort pulses at any desired wavelength would greatly increase their applicability to studies of nonlinear optical effects, lifetime measurements, etc. Work has also been conducted on flashlamp pumped dye lasers and such lasers have been successfully operated. It is anticipated that this type of laser will be useful for mode-locking and other experiments involving nonlinear gain processes.

Section 1

INTRODUCTION

Q-switched laser pulses have found wide application in diverse areas of pure and applied research. Some fields which have been opened to investigation by the availability of such pulses include gas breakdown at optical frequencies, optical plasma production for thermonuclear research, optical harmonic generation, stimulated scattering processes and optical coherency effects. Q-switched pulses have also been used for ranging and guidance systems, high speed photography, medical research, precision machinery, and other applications. The minimum pulse durations obtainable with the various existing Q-switching techniques are limited to approximately 10^{-8} seconds because of the requirement that one or more passes of the radiation through the laser medium are needed to build up the laser pulse.

The first paper describing the possibility of generating picosecond laser pulses was presented at the 1966 Quantum Electronics Conference. In the two years since this conference, the following advances in the generation of short, intense laser pulses have been achieved: 1.) a four to five order of magnitude decrease in pulse durations, from 10^{-8} sec to less than 10^{-12} seconds, 2.) a three order of magnitude increase in pulse power from 10^{9} watts to 10^{12} watts, 3.) a three order of magnitude increase in the resolution of detector systems, from 10^{-10} seconds to 10^{-13} seconds. It is to be expected that these developments should open more areas of investigation and should lead to additional scientific, military and commercial applications. The short time duration should allow the investigation of atomic processes that occur on a time scale that was previously inaccessible to direct observation. Coherency effects such as self-induced transparency might also be fruitfully investigated with ultrashort pulses. In addition, such pulses should have application to ranging and related problems. The use of an optical pulse of 10^{-11} seconds duration would allow the measurement of distances of miles to an accuracy of centimeters. Further, the high power available with such pulses will allow the investigation of nonlinear effects that were previously unobservable.

During the last two years the Research Laboratories of United Aircraft Corporation have been conducting a variety of government and corporate sponsored programs concerned with the generation, detection and measurement of ultrashort optical pulses and the investigation of their interaction with matter. Accomplishments under the subject contract have been described in the preceding summary section. In addition, it has been found possible a.) to generate and measure pulses as short as 4×10^{-13} seconds from a Nd:glass laser and 2×10^{-12} seconds from a ruby laser, b.) to generate electrical pulses of 90×10^{-12} seconds risetime, 65 volt amplitude and 500 MHz repetition rate, c.) to generate ultrashort acoustic pulses having harmonic content up to 7.4 GHz, d.) to generate and amplify single ultrashort pulses to peak powers of 10^{11} watts cm^{-2}, e.) to conduct a variety of experiments using short pulses for nonlinear optical experiments such as harmonic generation, stimulated scattering effects, self-trapping and multiple photon absorption.

Section 2

PROPAGATION CHARACTERISTICS OF ULTRASHORT PULSES

2.1 Introduction

Recent advances in laser technology have led to the production of coherent optical pulses having durations from the nanosecond regime down to 10^{-12} seconds.[1] Such time intervals are comparable to or shorter than the relaxation times associated with the energy levels of many atomic systems. The interaction of radiation and matter on such short time scales gives rise to new phenomena which can not be described by the rate equation analysis used previously[2] for much longer pulses.

Whenever it becomes necessary to extend the range of a theory to encompass new phenomena, it is useful to seek limiting cases of the new formalism[3,4,5] which will admit of exact solution. The purpose of the present work is to exhibit a model which is exactly soluble in regard to certain aspects of ultrashort pulse propagation. The model describes a number of effects which have been observed both experimentally[4,6] and as output from machine computations based upon more complete theoretical descriptions.[4,5] Hence it is felt that the model preserves many essential features of the processes which take place.

Although the coupling between radiation and matter is too strong to be treated by perturbation theory, a fairly extensive analysis of the model is still possible since it expresses this interaction in terms of a single nonlinear partial differential equation which arose long ago in differential geometry. Therefore, techniques developed about the turn of the century for the solution of such equations may be employed here to great advantage.

2.2 Basic Equations

We begin by summarizing the semiclassical description of the interaction of radiation with an assembly of two-level systems. The electric field $E(\underset{\sim}{r}, t)$ of a plane polarized optical pulse satisfies the usual wave equation

$$\nabla^2 E - \frac{1}{c^2}\frac{\partial^2 E}{\partial t^2} = \frac{4\pi n_0}{c^2}\frac{\partial^2 p}{\partial t^2} \qquad (2\text{-}1)$$

where c is the velocity of light in the medium, p is the polarization of an individual two-level system and n_0 is the number density of such systems.

The response of a two-level system to the optical field is described by equations for the density matrix of a two-level system which are similar to the Bloch equations of nuclear magnetic resonance,[7,8] i.e.

$$i\hbar\left(\frac{\partial \rho_{aa}}{\partial t} + \gamma_a \rho_{aa}\right) = V\left(\rho_{ba} - \rho_{ab}\right) \tag{2-2a}$$

$$i\hbar\left(\frac{\partial \rho_{ab}}{\partial t} + \gamma_{ab} \rho_{ab}\right) - \hbar\omega_{ab}\rho_{ab} = V(\rho_{bb} - \rho_{aa}) \tag{2-2b}$$

plus another pair of equations that are obtained from Eqs. (2-2) by interchanging a and b. In Eqs. (2-2) γ_a is the decay rate or longitudinal relaxation time of the upper laser level, γ_{ab} is the transverse relaxation time of dephasing time for levels a and b, ω_{ab} is the transition frequency and ρ_{aa}, ρ_{ab} etc. are the elements of a density matrix for a single two-level system. It is assumed that the optical field is coupled to the two-level systems through the usual dipole approximation so that V, the matrix element of the interaction potential between states a and b, is of the form

$$V = -\wp E \tag{2-3}$$

where $\wp$ is the dipole matrix element connecting these two levels.

The polarization of a two-level system is expressed in terms of the off-diagonal elements of the density matrix by [8]

$$P = -\wp(\rho_{ab} + \rho_{ba}) \tag{2-4}$$

while the population difference is $n_0\rho$ where ρ is related to the diagonal elements through

$$\rho = \rho_{aa} - \rho_{bb} \tag{2-5}$$

From Eqs. (2-2) and the definitions given in Eqs. (2-4) and (2-5), one finds that ρ and P are governed by the equations[9]

$$\frac{\partial \rho}{\partial t} = -\frac{2V}{\hbar \omega_{ab} P} \frac{\partial P}{\partial t} \tag{2-6}$$

$$\frac{\partial^2 P}{\partial t^2} + \omega_{ab}^2 P = \frac{2\omega_{ab} \mathcal{P}}{\hbar} V\rho \quad . \tag{2-7}$$

The relaxation rates γ_a, γ_b, γ_{ab} have been set equal to zero in these last two equations since we shall henceforth specialize the analysis to the ultrashort pulse limit in which pulse durations are short compared to all relaxation times.

However, since even the shortest pulses produced to date contain many optical cycles, it is appropriate to write the electric field in terms of a carrier wave, an envelope function $\mathcal{E}(\underset{\sim}{r},t)$ which varies slowly on the length and time scales of the carrier wave and a characteristic amplitude E_0. Hence we write

$$E(\underset{\sim}{r},t) = E_0 \mathcal{E}(\underset{\sim}{r},t) \cos(\underset{\sim}{k}_0 \cdot \underset{\sim}{r} - \omega_0 t) \, . \tag{2-8}$$

An additional unknown phase term could be included in the carrier wave. However, is is found[10] to be unnecessary for many aspects of the problem and will be neglected here. Because of the assumption that $\mathcal{E}(\underset{\sim}{r},t)$ varies slowly compared to the carrier wave, only first derivatives of $\mathcal{E}(\underset{\sim}{r},t)$ need be retained on the left-hand side of Eq. (2-1) when it is expressed in terms of the envelope function. On the right-hand side of Eq. (2-1) one may replace $\partial^2 P/\partial t^2$ by $-\omega_0^2 P$. In general, it is appropriate to consider not a single transition frequency ω_{ab} but a spread in transition frequencies about ω_{ab}. It is also convenient to assume that this distribution is symmetric about ω_{ab} and that the carrier frequency of the optical pulse is at this frequency, i.e., $\omega_0 = \omega_{ab}$.

Equation (2-1), specialized to a plane wave travelling in a positive x direction now becomes

$$\left(\frac{\partial \mathcal{E}}{\partial t} + c\frac{\partial \mathcal{E}}{\partial x}\right) \sin(k_0 x - \omega_0 t) = \frac{2\pi\omega_0 n_0}{E_0} \int_{-\infty}^{\infty} d\Delta\omega \, g(\Delta\omega) \, p(\Delta\omega, x, t) \tag{2-9}$$

where $\Delta\omega = \omega - \omega_0$ and

$$\int_{-\infty}^{\infty} d\Delta\omega g(\Delta\omega) = 1 \tag{2-10}$$

The formal solution of Eq. (2-7), with ω_{ab} now replaced by ω, may be written

$$p(\Delta\omega,x,t) = -2\wp\Omega\int_{-\infty}^{t} dt' \sin\omega(t-t')\rho(\Delta\omega,x,t')\mathcal{E}(x,t')\cos(k_0x-\omega_0t') \tag{2-11}$$

where $\Omega = E_0\wp/\hbar$. This expression for the polarization may be readily decomposed into parts which are in phase and $\pi/2$ out of phase with the electric field. One finds

$$p = \wp\left[P(\Delta\omega,x,t)\sin(k_0x-\omega_0t) + Q(\Delta\omega,x,t)\cos(k_0x-\omega_0t)\right] \tag{2-12}$$

in which

$$P = \Omega\int_{-\infty}^{t} dt'\mathcal{E}(x,t')\rho(\Delta\omega,x,t')\cos\Delta\omega(t-t') \tag{2-13}$$

$$Q = -\Omega\int_{-\infty}^{t} dt'\mathcal{E}(x,t')\rho(\Delta\omega,x,t')\sin\Delta\omega(t-t') \ . \tag{2-14}$$

In obtaining this result, terms near the second harmonic of ω_0 have been discarded. The functions P and Q are readily shown to satisfy the differential equations

$$\frac{\partial P}{\partial t} = \Omega\mathcal{E}\rho + \Delta\omega Q \tag{2-15}$$

$$\frac{\partial Q}{\partial t} = -\Delta\omega P \ . \tag{2-16}$$

When time dependence near the second harmonic of ω_0 is neglected in Eq. (2-6) it takes the form

$$\frac{\partial \rho}{\partial t} = -\Omega \mathcal{E} P . \tag{2-17}$$

With the transformation

$$\tau = \Omega (t - x/c) , \quad \xi = (\delta \Omega / c) x \tag{2-18}$$

where

$$\delta \equiv n_0 \hbar \omega_0 / (E_0^2 / 2\pi) . \tag{2-19}$$

Eqs. (2-9), (2-15), (2-16) and (2-17) become

$$\frac{\partial \mathcal{E}}{\partial \xi} = \int_{-\infty}^{\infty} d\Delta\omega\, g(\Delta\omega) P(\Delta\omega, \xi, \tau) \tag{2-20}$$

$$\frac{\partial \rho}{\partial \tau} = -\mathcal{E} P \tag{2-21a}$$

$$\frac{\partial P}{\partial \tau} = \mathcal{E} \rho + \frac{\Delta\omega}{\Omega} Q \tag{2-21b}$$

$$\frac{\partial Q}{\partial \tau} = -\frac{\Delta\omega}{\Omega} P . \tag{2-21c}$$

Equations (2-21) describe how the electric field $\mathcal{E}$ determines P, Q and ρ for a two-level system that is off resonance by an amount $\Delta\omega$. Equation (2-20) shows how the polarization due to a distribution of such systems reacts back on the electric field.

2.3 Reduction of the Basic Equations

It is interesting to note that Eqs. (2-21) are a set of scalar equations which have exactly the same structure as the Frenet-Serret equations of differential geometry.[11] It is known that the solution to such a set of equations can be made to rest upon the solution of a Riccati equation.[12] To show this, one first observes that an integral of Eqs. (2-21) is readily obtained in the form

$$\rho^2 + P^2 + Q^2 = 1 \tag{2-22}$$

in which an arbitrary function of ξ has been set equal to unity since before the arrival of the pulse $P=Q=0$ and $\rho^2=1$.

Two new functions are now introduced by writing

$$\frac{\rho+iP}{1-Q} = \frac{1+Q}{\rho-iP} = \phi \tag{2-23}$$

$$\frac{\rho-iP}{1-Q} = \frac{1+Q}{\rho+iP} = -\frac{1}{\psi} = \phi^* . \tag{2-24}$$

One then finds

$$\rho = \frac{1-\phi\psi}{\phi-\psi} \tag{2-25a}$$

$$P = i\frac{1+\phi\psi}{\phi-\psi} \tag{2-25b}$$

$$Q = \frac{\phi+\psi}{\phi-\psi} . \tag{2-25c}$$

Equations governing the time dependence of ϕ and ψ are readily deduced by inserting Eqs. (2-25) into Eqs. (2-21). It is found that ϕ satisfies the Riccati equation

$$\frac{\partial \phi}{\partial \tau} = i\xi\phi + \frac{1}{2}\frac{\Delta\omega}{\Omega}(\phi^2-1) \tag{2-26}$$

and that Ψ also satisfies this equation.

It was shown by McCall and Hahn[4] that one may obtain simple analytic expressions for the response of a two-level system to a field profile having the shape of a hyperbolic secant. This may be seen within the present formalism since the equation

$$\frac{\partial \phi}{\partial \tau} = i(2\,\mathrm{sech}\,t)\phi + \frac{i}{2}\,\frac{\Delta\omega}{\Omega}\,(\phi^2 - 1) \tag{2-27}$$

has the solution

$$\phi = \frac{f^2 + e^{i\sigma}}{2f\sin(\sigma/2) - (1+f^2)} \tag{2-28}$$

where $f = \Delta\omega/\Omega$ and

$$\sigma = 2\int_{-\infty}^{\tau} d\tau' \,\mathrm{sech}\,\tau = 4\tan^{-1} e^{\tau}. \tag{2-29}$$

According to Eqs. (2-25), the response of the system is

$$P = -\frac{\sin\sigma}{1+f^2} \tag{2-30a}$$

$$Q = \frac{2f\sin(\sigma/2)}{1+f^2} \tag{2-30b}$$

$$\rho = \frac{2\sin^2(\sigma/2)}{1+f^2} - 1\,. \tag{2-30c}$$

In general, one may carry out the usual transformation of the Riccati equation to a second-order linear equation. The problem may then be reduced to solving the equation

$$\ddot{w} + \frac{1}{4}(f^2 + \xi^2 + 2i\dot{\xi})w = 0 \tag{2-31}$$

where w is related to ϕ through the transformations $w = u \exp\left(-\frac{i}{2}\int_{-\infty}^{\tau} d\tau' \xi\right)$, $\phi = (2i/f)\, d(\ln u)/d\tau$. Equation (2-31) is particularly instructive since it puts power broadening in evidence.

However, from the well-known properties of these equations, it follows that in general it is impossible to write ϕ or ψ explicitly in terms of quadratures of ξ .

2.4 Specialization to a Soluble Model

If we consider the case of vanishing bandwidth, i.e.,

$$g(\Delta\omega) = \delta(\Delta\omega) \tag{2-32}$$

then only the case $\Delta\omega = 0$ need be considered in Eq. (2-26). Pulse propagation in a medium having a vanishing bandwidth is still possible due to the presence of power broadening.[13]

The equation for ϕ is now linear and the solution is

$$\phi = \pm e^{i\sigma} \tag{2-33}$$

where σ is given by

$$\xi = \frac{\partial \sigma}{\partial \tau} . \tag{2-34}$$

The ambiguity of sign in Eq. (2-33) is related to the two possible initial conditions $P(\xi, -\infty) = \pm 1$. The lower sign is associated with a medium that is initially in the lower level and is the one to be treated subsequently. This minus sign will we suppressed by incorporating it into the constant defined in Eq. (2-19).

From Eq. (2-25b) there follows

$$P = \sin\sigma \tag{2-35}$$

and Eq. (2-20) takes the form

$$\frac{\partial^2 \sigma}{\partial \xi \partial \tau} = \sin \sigma \ . \tag{2-36}$$

This nonlinear partial differential equation is the fundamental equation of the model.[14] Fortunately, it has already been studied extensively since it arose in the theory of surfaces of constant negative curvature.[15] The general solution of the equation is not known. However, particular solutions may be obtained since the equation is of a type for which a Baecklund transformation[16] may be devised. This transformation theory enables one to relate pairs of solutions of certain partial differential equations. The transformation equations for Eq. (2-36) are[15]

$$\frac{1}{2} \frac{\partial}{\partial \tau} (\sigma_1 - \sigma_0) = a_1 \sin\left(\frac{\sigma_1 + \sigma_0}{2}\right) \tag{2-37a}$$

$$\frac{1}{2} \frac{\partial}{\partial \xi} (\sigma_1 - \sigma_0) = \frac{1}{a_1} \sin\left(\frac{\sigma_1 + \sigma_0}{2}\right) \tag{2-37b}$$

where a_1 is an arbitrary constant. According to Eqs. (2-37), if σ_0 is a known solution of Eq. (2-36), another solution σ_1 may be obtained by solving this pair of first-order equations.

2.5 Particular Solutions

By inspection one sees that a solution of Eq. (2-36) is

$$\sigma_0 = 0 \ . \tag{2-38}$$

It then follows from Eqs. (2-37) that

$$\sigma_1 = 4 \tan^{-1} e^{a_1 \tau + \xi / a_1} \tag{2-39}$$

is another particular solution. By Eq. (2-34), the pulse envelope has the form

$$\mathcal{E}_1 = \operatorname{sech} \frac{1}{2} \Omega (t - x/v) \tag{2-40}$$

where

$$v = c/(1 - 4\delta) \tag{2-41}$$

The constant a_1 has been chosen so as to normalize $\mathcal{E}$.

It has been shown[4] that an extremely useful function in the study of ultrashort pulses is the area function $\theta(x)$ which is defined as

$$\theta(x) \equiv \Omega \int_{-\infty}^{\infty} dt\, \mathcal{E}_1(x,t) \tag{2-42}$$

For the envelope obtained above, one finds $\theta = 2\pi$. It has become customary to borrow from the terminology of nuclear magnetic resonance and refer to $\mathcal{E}_1$ as a 2π pulse. It is now also known[4] that the area function for a 2π pulse is not a stable quantity unless the two-level systems are initially in the ground state. In this case the pulse shape given in Eq. (2-40) corresponds to the recently discovered self-induced transparency effect.[4]

The determination of σ_1 from σ_0 required the integration of two first-order equations. It is known[17] from the theory of surfaces of constant negative curvature that there exists a relationship among four solutions of Eq. (2-36) which does not involve quadratures. Although this relationship is usually derived by appeal to the geometric significance of the analysis, for present purposes it may be more conveniently obtained by introducing the following symbolic representation of the transformation equations (2-37).

A transformation from a solution σ_i to a solution σ_j with a constant a_k will be represented as shown in Fig. 1. Now the above-mentioned relationship involving four solutions is

$$\tan\left(\frac{\sigma_3 - \sigma_0}{4}\right) = \frac{a_1 + a_2}{a_1 - a_2} \tan\left(\frac{\sigma_1 - \sigma_2}{4}\right). \tag{2-43}$$

It may be shown quite easily that the equations corresponding to the sequence of transformations depicted in Fig. 2 can be combined to yield this purely trigonometric relation.

If one again assumes $\sigma_0=0$, the final solution σ_3 in Eq. (2-43) may be made to vary from -2π to 2π as τ varies from $-\infty$ to ∞. One need only require $a_1 - a_2 > 0$. Such a solution will represent a 4π pulse. In order to obtain a pulse shape which contains only one peak as a function of time at x=o, one may impose the additional requirement $\partial^2\xi/\partial\tau^2<0$ at $\xi=\tau=0$. This leads to the inequality

$$(a_1+a_2)(a_1^2+a_2^2+3a_1a_2)>0\,. \tag{2-44}$$

If one also requires $\xi(0,0)>0$ and arbitrarily sets $a_2=-1$, then the inequality is equivalent to $\frac{1}{2}(3+\sqrt{5})\le a_1<\infty$. In terms of the angle defined by $a_1=(1+\sin\theta)/\cos\theta$, this condition takes the form $\cos^{-1}(2/3)\le\theta<\pi/2$.

The pulse shape is given by[18]

$$\xi(x,t)=\frac{2\sin\theta\left[\operatorname{sech}\Omega(t-x/v)+a\operatorname{sech}a\Omega(t-x/v')\right]}{1-\cos\theta\left[\tanh\Omega(t-x/v)\tanh a\Omega(t-x/v')-\operatorname{sech}\Omega(t-x/v)\operatorname{sech}a\Omega(t-x/v')\right]} \tag{2-45}$$

where $v'=c/(1-\delta/a^2)$, $v=c/(1-\delta)$. An example for $\theta=\cos^{-1}(2/3)$, $\delta=-1/2$ is shown in Fig. 3. It is of interest to note that when the two pulses are completely separated, only the leading one retains any information about the initial pulse shape.

The procedure outlined above may be generalized to yield expressions for any $2n\pi$ pulse where n is a positive integer. As an example, the 6π pulse is obtained from the sequence of transformations depicted in Fig. 4. Certain constraints may be immediately imposed upon the triad of constants a_1, a_2, a_3. Firstly, for the envelope function corresponding to σ_2 to be positive, one requires $a_2>0$. One then proceeds to make σ_a a 4π pulse which in addition requires $a_1<0$ and σ_b is made a zero π pulse which is obtained by requiring $0<a_3<a_2$. Additional restrictions are required in order to assure a pulse shape which consists of a single peak at x=o. The inequality is much more complicated in this case than in Eq. (2-44) and has not been analyzed in detail. By a simple trial-and-error method the case shown in Fig. 5 has been obtained. Again it is found that the last pulse is insensitive to variations in the initial pulse shape. This effect has been observed experimentally.[19]

2.6 Stability of Pulse Shapes

The pulse shapes calculated above will not bear any relation to those realizable in nature unless they are stable with respect to perturbations about these shapes. In the present section a specific example will be used to show that an infinitesimal amount of phenomenological damping is necessary in order for the pulse shape to be stable.

To exhibit the instability of the undamped solutions, we first consider a perturbation to the solution given in Eq. (2-39) and write

$$\sigma(u,v) = 4\tan^{-1}e^{u} + \sigma^{(1)}(u,v) \tag{2-46}$$

where new variables

$$\begin{aligned} u &= a\tau + \xi/a \\ v &= a\tau - \xi/a \end{aligned} \tag{2-47}$$

have been introduced. We shall perform only a linear stability analysis which leads to the following equation for the perturbation $\sigma^{(1)}$.

$$\frac{\partial^2\sigma^{(1)}}{\partial u^2} - \frac{\partial^2\sigma^{(1)}}{\partial v^2} - (1 - 2\,\mathrm{sech}^2 u)\sigma^{(1)} = -2a\,\mathrm{sech}\,u\,. \tag{2-48}$$

Particular solutions of this equation are readily obtained in the product form $\sigma^{(1)} = U(u)V(v)$. The solution of the equation for V is immediate, while the form of the equation for U is that of a Schroedinger equation for a sech^2 potential. Such an equation may be analyzed completely.[20] The simplest eigenfunction is

$$U(u) = \mathrm{sech}\,u. \tag{2-49}$$

One then finds that a possible perturbation is

$$\sigma = (A + Bv)\,\mathrm{sech}\,u = \left[A + B(u - 2x)\right]\mathrm{sech}\,u\,. \tag{2-50}$$

This perturbation may be interpreted as a disturbance which propagates at the

velocity of the zero-order pulse but contains a contribution that grows linearly with distance. Hence the undamped solution is seen to be unstable although the growth of the perturbation in this case is only linear.

The stability of solutions in the presence of damping may be indicated by considering the equation

$$\frac{\partial^2 \sigma}{\partial \xi \partial \tau} + k \frac{\partial \sigma}{\partial \tau} = \sin \sigma \qquad (2\text{-}51)$$

which is the counterpart of Eq. (2-36) when damping is included in Eq. (2-1). While the steady state solution will now differ slightly from the solution given in Eq. (2-39), the perturbation may be analyzed as before. It is now found that the term V(v) satisfies the equation

$$(v'' - kv')/v = \text{constant} \qquad (2\text{-}52)$$

which gives rise to an exponential decay of the perturbation as it propagates in the positive x direction.

Section 3

MEASUREMENT OF NANOSECOND FLUORESCENCE DECAY TIMES

The simplest type of lifetime determination is the measurement of a fluorescence decay time. Since the early 1930's it has been possible to measure fluorescence lifetimes as short as one nanosecond.[22] However, the fluorometers devised for these measurements are complex and cumbersome. Moreover, insomuch as the actual decay curve is not observed, the measurements are indirect. This latter deficiency leads to serious problems when competing channels of decay are in evidence. Therefore, a simpler and more direct technique for measuring rapid fluorescence decay rates is desirable.

To observe a fluorescent decay, a high-intensity source having a rapid fall time is required to excite the fluorescence and a wide bandwidth detection system is needed to detect it. Mode-locked lasers are an ideal excitation source. A number of different lasers have been successfully mode-locked. Of these, the simultaneously Q-switched and mode-locked ruby[23] or neodymium[48] lasers offer the greatest peak output power. For materials absorbing in the blue end of the spectrum rather than in the red, frequency doubling may be employed with these lasers. In addition to the pulsed phase-locked lasers, the argon laser[24] and the Nd^{+3}: YAG laser[25] have been continuously mode-locked with appreciable peak output power. In all of the above lasers, the widths of the output pulses are considerably less than one nanosecond.

With the continuously mode-locked lasers, a crossed-field photomultiplier[26] used in conjunction with a sampling oscilloscope could give an overall detection risetime as short as 0.06 nanosecond. Such a system could equal even the fastest modern fluorometer[27]. With the pulsed mode-locked lasers, a traveling wave oscilloscope must be used. These typically have a risetime of on the order of a few tenths of a nanosecond.

In the present case a simultaneously Q-switched and mode-locked ruby laser was used to excite the fluorescence. A UARL 1240 Phototransducer having a 0.3 ns risetime was used to detect the fluorescence radiation. The output from this detector was displayed on a Tektronix 519 oscilloscope. Figure 6a shows an oscilloscope tracing of the laser output. The pulse widths shown illustrate the time response of the detection system.

Two classes of dyes were investigated in this experiment, those excited directly by the ruby laser and those excited by the second harmonic of ruby. The former were the dyes commonly used for Q-switching the ruby laser, while the latter dyes were, for the most part, liquid laser dyes[28,29]. The experimental arrangement used for the liquid laser dyes is shown in Fig. 7. A copper sulfate solution was used to absorb the scattered laser light, while a sharp cut interference

filter was used to block the scattered second harmonic light. In that way only the fluorescence was detected by the photodiode. In all cases the concentrations of the dyes were adjusted to give a transmission through the 1-cm dye cell of approximately 10% at 3470 Å.

A typical oscilloscope tracing of a fluorescence is shown in Fig. 6b. The decay times for the various dyes were determined by fitting an exponential to each of the decaying portions in the oscillographs. For each dye the results from two such photographs (i.e., ten curves) were then averaged together. The results for the liquid laser dyes are summarized in Table I. The values given for the lifetimes should be accurate to better than ± 20%.

The setup used for determining the fluorescence lifetime of the Q-switching dyes was quite similar to that used for the liquid laser dyes. Of course, since the Q-switching dyes are excited directly by the laser beam, frequency doubling was not necessary. To detect the fluorescence, an S-1 version of the UARL 1240 photodiode was used. A Corning Glass Works CS-7-69 filter was used to separate the scattered laser light from the fluorescence.

Three Q-switching dyes were investigated, chloro-aluminum phthalocyanine, vanadyl phthalocyanine, and cryptocyanine. In the case of the phthalocyanines, the lifetimes were measured in several solvents. The concentrations were adjusted for a transmission of about 10% at 6943 Å through the 1-cm-thick dye cell. In the case of chloro-aluminum phthalocyanine in ethanol, the concentration was varied to give a transmission of from 4% to 75% to determine if the lifetime depended on concentration. No such dependence was found. The results are summarized in Table II.

The fluorescent decay in cryptocyanine was by far the most rapid. The measurement there was limited by the detection system response time. Spaeth and Sooy[30] have estimated a decay time of 4×10^{-11} seconds for cryptocyanine in propanol. It is quite possible that the fluorescence decay time in a methanol solution is as short. The lifetime measured for chloro-aluminum phthalocyanine in 1-chloronaphthalene is somewhat longer than reported by Bowe, et al.[31] though the difference is only 0.1 ns outside of the experimental errors. The result for vanadyl phthalocyanine in nitrobenzene is in good agreement with that obtained by Arecchi, et al[32].

Section 4

LIGHT AMPLIFICATION IN SATURABLE ABSORBERS WITH PICOSECOND PULSES

4.1 Introduction

In the previous section a technique for the determination of lifetimes through the observation of fluorescence decay was described. It is of considerable interest to measure the recovery times of the dyes used as saturable absorbers in mode-locked lasers. A large number of these dyes are fluorescent and their recovery times could be inferred from a measurement of the fluorescent decay time. It is also possible to measure the recovery time directly by exciting the dye with a strong saturating pulse followed by a weak probing pulse. If the relative time delay of the weak pulse is adjustable, it can be used to monitor the recovery of the absorption of the dye after the saturating pulse. Fluorescence measurements are limited by the risetime of the electronics that are involved. The second, direct method should be capable of measuring much shorter recovery times. An experimental program to use this technique to measure recovery times in saturable absorbers was initiated. During the course of these experiments a new nonlinear effect was discovered. This effect has been termed Light Amplification in Saturable Absorbers (LAISA).

It was found that an absorber, driven into saturation by an intense light pulse from a mode-locked ruby laser, can amplify a weaker light pulse simultaneously incident upon the medium. Energy gains as high as 20 times were observed with a path length of only 1 cm. in the saturable absorbing dye solution. A theory giving qualitative agreement with the experimental results has been developed. The effect has an important bearing on the subject of mode-locking with saturable absorbers.

This result is quite similar to that reported by Senitzky, Gould and Cutler for microwave saturable absorbers.[33] Gain in saturable absorbers is closely related to spectral hole burning. Previous theoretical[34] and experimental[35,36] investigations of hole burning in saturable absorbers have indicated that the weak wave attenuation is merely reduced over that for the strong wave, that is to say, that the hole in the absorption spectrum reaches only to the zero attenuation point. The fact that weak wave amplification can be achieved means that the hole in the absorption spectrum actually penetrates through to the negative absorption region. As will be shown this has an important bearing on the behavior of a laser mode-locked by a saturable absorber.

In Section 4.2 the experimental evidence illustrating gain is presented. The data shown is for cryptocyanine in methanol. In Section 4.3 a theory is given for the effect. Using a two-level model for the dye, qualitative agreement with the experimental results is obtained. The improvements required to allow a quantitative comparison between theory and experiment are also discussed. In Section 4.4 the connection between the gain phenomenon and the ability of a

dye to bring about mode-locking in a laser cavity is discussed. Probably the most important consequence of this interconnection is the fact that because of the gain it ought to be possible to obtain mode-locked pulses shorter in duration than the reciprocal gain bandwidth of the laser medium.

4.2 Experimental Results

The experimental arrangement used to study gain in saturable absorbers is shown in Fig. 8. Two beams, one very intense and the other relatively weak, are incident on the dye cell. The weaker, probing beam is derived by reflection as shown. Unwanted reflections were avoided by the use of wedges. In most of the experiments performed the spacing between the reflecting wedge and the dye cell was such as to impart a 2 picosecond delay to the probing beam. This is small compared to the measured average pulse duration of 25 picoseconds. The output of the photodiode (UARL 1240) is displayed on a Tektronix 519 oscilloscope.

When the dye cell is filled with just methanol an oscilloscope trace like that shown in Fig. 9a is obtained. The first pulse in each pair measures the energy in the intense, saturating pulse while the second monitors the energy in the weaker probing pulse. The pulse heights were made equal by adjusting the positions of the two pieces of ground glass shown in Fig. 8. The addition of an absorbing dye to the methanol should decrease the height of the second pulse relative to the first. The fractional attenuation would be just the ratio of the two pulse amplitudes.

Fig. 9b shows the result when cryptocyanine is added to the methanol. In this case the concentration of the dye solution was adjusted to give a low level transmission of 1 part in 10^5 (optical density 5.0) at 6943 Å. It is clear from this photograph that the probing beam is actually amplified during the initial portion of the pulse train. The drop-off in amplification further along in the pulse train is typical. The amount of gain is dependent on the concentration of the dye, increasing from 2 to 3 in an optical density 0.3 solution to 10 to 20 in an O.D. 10.0 solution. Also important in determining the gain is the delay time in the probing pulse. The gain decreases rapidly as the delay is increased beyond the pulse duration. Curiously, at least for lower concentration solutions the gain decreases only slightly if the incident intensity is reduced from the 1 GW/cm^2 level used for most of these measurements to 250 Mw/cm^2.

Several other important features of the gain effect are brought out by far field patterns of the beams passing through the dye cell. These are shown in Figs. 9c and 9d. (O.D. 1.0 solution). Amplification of the probing beam is obvious in comparing the two photographs. Also obvious is the generation of a third beam in the amplification process. The generation in this beam is critically dependent on the angular separation, θ , between the saturating beam and the probing beam. This is illustrated in Fig. 10 (O.D. 1.0 solution). For the larger angular separations ($\theta \cong 20$ milliradians) a third beam is not produced. Gain in the probing beam persists with a gradual fall-off to 50 milliradians and

beyond. With decreasing angular separations the generation in the third beam increases until at θ = 7 mrad., the energy in the third beam is about equal to that in the amplified probing beam.

Preliminary spectroscopic measurements have also been made of the various beams passing through the cell. These measurements are only precise enough to show that there are no gross (> 50 cm^{-1}) frequency shifts in any of the beams. More accurate measurements are in progress.

Many of the experiments performed using cryptocyanine in methanol have also been carried out using other saturable absorbers. Gain has been observed in acetone, methanol and dimethyl sulfoxide solutions of cryptocyanine, dicyanine A and 1,1'-diethyl-2,2'-dicarbocyanine iodide. Chloro-aluminum phthalocyanine in ethanol also exhibits gain. On the other hand no effect was observed in linear absorbers like copper sulfate in water.

4.3 Theoretical Considerations

The great similarity between the angular dependence shown in Fig. 10 and that predicted for light by light scattering[37] strongly suggests that a non-linearity in the refractive index is responsible for the gain observed here. However, it must be remembered that no effect was observed with the solvent alone and that the concentration of the dye in the solution was generally on the order of 10^{-5}M. The low dye concentration makes it unlikely that an index effect is the origin of the gain. In fact, the dye would have to have a molecular Kerr constant 1000 times larger than nitrobenzene to account for the gains observed.

Also suspect as a source for the gain are coherency effects of the sort reported by Hahn and McCall[38]. While the pulses are of sufficient intensity for such effects to come into play, the pulse durations are believed to be long in comparison to the phase memory time. The fact that the gain vanishes when the saturating and probing pulses are separated in time supports this view. It is also difficult to understand the observed angular dependence in the context of a coherency phenomenon. Despite these objections, coherency may still play a role in the gain effect, but it is unlikely that it plays the dominant role.

The fact that gain occurs in every saturable dye examined suggests that the effect is interrelated with the saturation itself. This same conclusion was drawn in the case of the microwave experiments[33]. In fact, using a density matrix formulation, the authors of the microwave work were able to show that the saturation of absorption can lead to the amplification of weaker beams simultaneously incident on the absorber. This formalism could readily be carried over to the optical region and to the case that the various beams are not collinear. However, a simpler and perhaps more physical treatment is possible. It is instructive to first review the problem of the absorption of a single monochromatic wave in a saturable absorber.

A field of the form

$$E = E_0 \cos(\omega_0 t - k_0 z) \tag{4-1}$$

incident upon a saturable absorber induces a polarization of the form

$$P = \chi'(I)\, E_0 \cos(\omega_0 t - k_0 z) + \chi''(I) E_0 \sin(\omega_0 t - k_0 z) \tag{4-2}$$

where $\chi'(I)$ and $\chi''(I)$ are the in phase and out of phase parts respectively of the susceptibility. Because the dye is saturable these susceptibilities are a function of the local intensity, $I = (c/4\pi)\langle E^2 \rangle$, where the brackets indicate a time average. Substitution of the above polarization into the appropriate Maxwell's equation leads to the following phase and amplitude equations:

$$k_0^2 - \frac{\omega_0^2}{c^2} = \frac{4\pi\omega_0^2 \chi'(I)}{c^2} \tag{4-3}$$

$$\frac{\partial E_0}{\partial z} = - \frac{2\pi\omega^2 \chi''(I)}{k_0 c^2} E_0 \, . \tag{4-4}$$

Because of the dependence of the susceptibilities on the intensity these equations are coupled. For the sake of simplicity and because it can frequently be neglected, this coupling is usually ignored . Equations (4-3) and (4-4) are then easily solved.

In the present case two waves are initially incident on the dye and a third is generated in it. The same treatment as carried out above can be used. For generality the three fields may be assumed to have different frequencies so that the total field is

$$E = E_0 \cos(\omega_0 t - \vec{k}_0 \cdot \vec{r} + \phi_0) + E_1 \cos\left[(\omega_0 + \Omega) t - \vec{k}_1 \cdot \vec{r} + \phi_1\right] + E_{-1} \sin\left[(\omega_0 - \Omega) t - \vec{k}_{-1} \cdot \vec{r} + \phi_{-1}\right] \tag{4-5}$$

where $E_0 >> E_1 , E_{-1}$ and $\vec{k}_0 = k_0 \hat{z}$, $\hat{z}$, being a unit vector in the Z-direction. If the coupling between the phase and amplitude equations is neglected, all that is needed to describe the growth or decay of the amplitudes is the out of phase polarization,

$$P = \left\{\chi''(I_0) + \frac{\partial \chi''(I)}{\partial I}\Big|_{I_0}\delta I\right\}\left\{E_0 \sin(\omega_0 t - \vec{k}_0\cdot\vec{r} + \phi_0) + E_1 \sin\left[(\omega_0+\Omega)t - \vec{k}_1\cdot\vec{r} + \phi_1\right] + E_{-1}\sin\left[(\omega_0-\Omega)t - \vec{k}_{-1}\cdot\vec{r} + \phi_{-1}\right]\right\} \tag{4-6}$$

where δI is the increase in intensity due to the addition of the weak fields, E_1 and E_{-1}, to the strong field, E_0. The field equations derived from this polarization are

$$\frac{\partial E_0}{\partial z} \cong -\alpha E_0 \tag{4-7a}$$

$$\frac{\partial E_1}{\partial z} \cong (\beta E_0^2 - \alpha)E_1 + \beta E_0^2 E_{-1}\cos(Kz + \Phi) \tag{4-7b}$$

$$\frac{\partial E_{-1}}{\partial z} \cong (\beta E_0^2 - \alpha)E_{-1} + \beta E_0^2 E_1 \cos(Kz + \Phi) \tag{4-7c}$$

where $\alpha = \frac{2\pi\omega_0\chi''}{c}$, $\beta = -\frac{\omega_0}{4}\frac{\partial\chi''}{\partial I}\Big|_{I_0}$, $\Phi = \phi_1 + \phi_{-1} - 2\phi_0$ and $K = (2k_0 - k_1 - k_{-1})\cdot\hat{z}$. These equations can be solved, if the attenuation of the saturating wave, E_0, is neglected. In many of the experiments performed the attenuation of the saturating beam was, in fact, negligible. With the initial conditions $E_1(z=0) = E_1^0$ and $E_{-1}(z=0) = 0$, the solutions are:

$$E_1(z) \cong E_1^0 e^{(\beta E_0^2 - \alpha)z}\cosh\left\{\beta E_0^2 \frac{\sin(Kz+\Phi) - \sin\Phi}{K}\right\} \tag{4-8a}$$

$$E_{-1}(z) \cong E_1^0 e^{(\beta E_0^2 - \alpha)z}\sinh\left\{\beta E_0^2 \frac{\sin(Kz+\Phi) - \sin\Phi}{K}\right\} . \tag{4-8b}$$

Several properties of these solutions are illustrated in Figs. 11 and 12 where a two-level system was assumed for the dye. Only the case $\Phi = 0$ is treated. Fig. 11 shows the power developed in the probing beam and in the generated beam as a function of the saturating intensity and of the dye concentration for a 1 cm. thick cell. The phase mismatch, K, was assumed to be zero. Fig. 11 does predict gain but the gain predicted is considerably less than that observed in every case.

Fig. 12 shows the variation of the gains with the degree of phase mismatch. Since $K = 2k_0 - k_1 \cos\theta_1 - k_{-1}\cos\theta_{-1}$, this figure also demonstrates the angular dependence of the gain. The predicted angular dependence can be compared with that observed experimentally by making use of the observed fact that $\theta_1 = \theta_{-1}$. If there is no frequency shift in any of the beams so that $k_0 = k_1 = k_{-1}$ then the gain fall-off in Fig. 12 is much too rapid. However, only a slight (0-1 cm^{-1}) frequency shift in the generated beam is needed to bring the predicted angular dependence into agreement with that observed experimentally.

In light of the many approximations needed to arrive at the results given in Eqs. (4-8a) and (4-8b) the lack of quantitive agreement with the experimental results is not surprising. Better agreement should be obtainable by taking into account transient effects, by using a better model for the dye than a two-level system and by including the coupling between the phase and amplitude equations. Unfortunately, adding in any one of these factors greatly complicates the analysis.

Before concluding this section, it should be noted that the treatment given above has a very simple interpretation in the case that two incident waves are collinear and of different frequency. The intensity in the saturable absorber is then amplitude modulated at the different frequency. Provided that the dye can respond to the modulation, the non-linear absorption of the dye will enhance and distort the modulation. This is illustrated graphically in Fig. 13. The distortion of the modulation indicates the generation of other frequency sidebands. The enhancement of the modulation arises because of reduced attenuation in the sidebands relative to the center frequency. Whether this becomes actual gain depends on the shape of the curve in Fig. 13 at the operating point and on the absorption at that point.

4.4 Mode-Locking and the Amplification Effect

It is, of course, clear that if gain can be demonstrated in a saturable dye outside the cavity of a mode-locked ruby laser, it must also take place in the dye used to mode-lock the laser. It is also likely that the amplification effect plays an important role in the mode-locking process. That this is so can be seen from Fig. 13. When many frequency modes are present, the relative phases are important in determining the amount of sideband gain in the dye. For example, the modes might be phased to produce a frequency modulated wave with little amplitude modulation. From Fig. 13 it can be seen that there would be little amplification. On the other hand, when the modes are phased for a maximum amplitude modulation, the sideband gain is also a maximum. The maximum amplitude modulation occurs in the mode-locked case.

The gain in a bleachable dye can also affect the duration of the output pulses of a laser mode-locked by such a dye. It is usually said that the shortest pulses obtainable from a mode-locked laser would have a duration equal to the reciprocal gain bandwidth of the laser medium. This is true only to the extent that the saturable dye is completely passive. Because of the fact that

sideband amplification can be obtained in such dyes, it may be possible to produce pulses shorter than the reciprocal gain bandwidth for the laser medium itself. It should be noted that the gain bandwidth for the dye is equal to its power broadened linewidth[33]. How effective this gain might be in shortening the pulses would depend on the magnitude of the gain, on the losses in cavity and on such other factors as dispersion. The fact that the gain varies from dye to dye suggests that different dyes might vary in their ability to produce short pulses in a laser system. Indeed, this has been found to be the case[39] but it has not yet been possible to show a correlation between the pulse duration obtained and the amount of sideband gain exhibited by the dye.

4.5 Conclusions

The simple theory outlined above succeeds in explaining the salient features of the experimental observations. However, if quantitive agreement between experiment and theory is to be expected substantial refinements must be made. Such refinements may prove difficult to incorporate into the present theory. A test of the basic premise of this theory, namely that the gain is a consequence of the non-linear absorbtivity of the saturable dyes, can be made by an experimental determination of the transfer function shown in Fig. 13. The experimental gain could then be compared with that derived directly from this curve. All such data should be obtained using a single mode-locked laser pulse to avoid complications arising from the transfer of population in the lowest singlet manifolds of the dye molecules to the triplet manifolds[36]. This transfer of population is believed to be responsible for the loss of gain toward the end of the pulse trains and for the lack of good reproducibility in the present results.

Section 5

INTERACTION OF INTENSE FREQUENCY-SWEPT LASER PULSES WITH MATTER

5.1 Theoretical Analysis

A theoretical investigation of the interaction of an intense frequency-swept pulse of light (i.e., an optical chirp) with matter has been conducted. The first interesting result to come out of the investigation was the adiabatic inversion of populations between a pair of levels when the frequency of the pulse is swept through their resonant frequency. The second result was the dependence of the phase of the induced polarization on the direction of the sweep. These effects have been observed in nuclear magnetic induction experiments (Ref. 40), and the new features in our experiments will be: (1) the use of electric dipole transitions, (2) excitation of the sample by a traveling wave. These are the two features that distinguish the so-called "photon" echo (Ref. 41) from the well-known spin echo experiments (Refs. 42, 43). In addition, the frequency is swept across the otherwise unperturbed resonance between the levels in our experiments, whereas in NMR the frequency is held fixed and the energy level spacing is swept by the external magnetic field.

The geometrical representation of the Schrodinger equation due to Feyman, et al (Ref. 44) provides a lucid description of the phenomenon. The Schrodinger equation

$$i\hbar\frac{\partial\psi}{\partial t} = H\psi = H_0\psi + V\psi \tag{5-1}$$

is rewritten

$$\frac{d\vec{r}}{dt} = \vec{\omega}\times\vec{r}, \tag{5-2}$$

where

$$\psi(t) = a(t)\psi_a + b(t)\psi_b. \tag{5-3}$$

For $m = \pm 1$ transitions, the following relationships hold for the parameters of Eqs. (5-1) and (5-2):

$$\hbar\omega_1 = V_{ab} + V_{ba} = -\gamma E_x, \tag{5-4a}$$

$$\hbar\omega_2 = i(V_{ab} - V_{ba}) = -\gamma E_y, \tag{5-4b}$$

$$\hbar\omega_3 = \hbar\omega_0 = E_b - E_a, \tag{5-4c}$$

$$r_1 = ab^* + a^*b, \tag{5-5a}$$

$$r_2 = i(ab^* - a^*b), \tag{5-5b}$$

$$r_3 = a^*a - b^*b \tag{5-5c}$$

where $\gamma = \mu_{ab}^{+} = \mu_{ba}^{-}$ is the dipole moment operator. The precession of $\vec{r}$ about the resultant $\vec{\omega}$ is completely analogous to the precession of the nuclear moment about a resultant magnetic field B.

For a pulse having the following electric field components

$$E_x = A(t) \cos \phi(t), \tag{5-6a}$$

$$E_y = A(t) \sin \phi(t), \tag{5-6b}$$

the picture is simplified by referring the vector $\vec{r}$ to a frame of axes rotating at a rate $\Omega(t) = d\phi/dt$ about the 3-axis. In the new frame

$$\frac{\vec{dr}'}{dt} = \vec{\omega}' \times \vec{r}', \tag{5-7a}$$

$$\hbar\omega_1' = -\gamma A(t) \tag{5-7b}$$

$$\omega_2' = 0,$$

and

$$\omega_3' = \omega_0 - \Omega(t). \tag{5-7c}$$

The vector $\vec{r}$ for an atom in the lower (or upper) state has $r_3 = 1$ (or -1) and $r_1 = r_2 = 0$.

The response of the quantum system to the chirped pulse is represented by the precession of the state vector $\vec{r}'$ about the resultant $\vec{\omega}'$ while the latter vector is tipped slowly (compared to the precession rate) through 180°. This is depicted in Fig. 14 where $d\Omega/dt$ and A are positive and the system is resonant at that $\Omega(t)$ where $A(t)$ is maximum. If $d\Omega/dt$ is constant, the curve of Fig. 14 has the same shape as the envelope $A(t)$. The semivertical angle of the cone of precession is approximately equal to the angle through which $\vec{\omega}'$ turns in the time that $\vec{r}'$ takes to precess 90° about the initial $\vec{\omega}'$. This is given by the relation:

$$\delta\theta \approx \frac{\pi\gamma\left(\frac{dt}{dt}\right)_o}{2\hbar\left[\omega_o - \Omega(0)\right]^2} + \frac{\pi^2\gamma\left(\frac{d^2A}{dt^2}\right)_o}{8\hbar\left[\omega_o - \Omega(0)\right]^3} . \tag{5-8}$$

Here the zero denotes conditions at the beginning of the pulse. Because the envelope $A(t)$ starts from zero and ends at zero, it is not necessary to sweep over a large range as in the corresponding NMR experiments where the rf field amplitude is kept constant.

The adiabatic condition (constant $\delta\theta$) is that the rate at which $\vec{\omega}'$ is tipped should be always small compared to the rate of precession of $\vec{r}'$ about $\vec{\omega}'$. Near the middle of the pulse this yields the relation

$$\gamma A_{max}/\hbar \gg \frac{\hbar\dot{\Omega}}{\gamma A_{max}} \tag{5-9a}$$

or

$$\dot{\Omega} \ll \left(\frac{\gamma A_{max}}{\hbar}\right)^2. \tag{5-9b}$$

Near the ends of the pulse the same condition yields

$$\frac{\Delta\Omega}{2} \gg \frac{2\gamma\left(\frac{dA}{dt}\right)_{max}}{\hbar\,\Delta\Omega} \tag{5-10a}$$

or

$$\left(\frac{dA}{dt}\right)_{max} \ll \frac{\hbar(\Delta\Omega)^2}{4\gamma}. \tag{5-10b}$$

An additional condition is that the pulse length ought to be short compared to the time between dephasing collisions.

The vector $\vec{r}'$ will follow either $\vec{\omega}'$ or $-\vec{\omega}'$, depending on whether the two vectors are initially parallel or antiparallel. The induced polarization is proportional to the component r_1, while the field is opposite to ω_1, so that the induced polarization will be in the same direction as the driving field if the frequency sweep is negative and the system is initially in its ground state. This will produce a decrease in pulse propagation speed. Reversing the sweep direction (or the population difference) produces a polarization 180° out of phase with the E-field, and this will have some effect (perhaps defocusing) on the stability of the propagating pulse.

5.2 Experiments

For the experimental attempt to observe these effects, we have built a CO_2 laser for generating optical chirps of 10.6 microns wavelength, 0.5 to 1.0 microsecond pulse duration and 60 MHz sweep, and will use this laser as a source for inverting the ν_3 vibration of sulphur hexafluoride (SF_6) between the ground and first excited states. Except for the chirp feature, the laser is of fairly standard design: water-cooled, external flat and spherical mirrors, sodium chloride Brewster windows, aperture stops for selection of dominant mode (TEM_{00n}). The laser configuration is shown in Fig. 15.

The frequency is swept by changing the optical cavity length. This is accomplished mechanically by rotating the flat mirror by a synchronous 1800 rpm

motor with an offset of a centimeter or two between the rotation axis and the laser axis. The cavity length of 150 cm provides a spacing of 100 Mc for the TEM_{oon} modes while the CO_2 line width is about 60 Mc. Figure 16 shows a set of pulses generated by this scheme. The 2 μsec spacing between the pulses corresponds to an offset of about 1.3 cm of the rotating mirror. The biggest pulse in the train occurs when the laser mode is on axis with the aperture stops.

The frequency sweep is produced by the motion of the mirror, which gives a time-dependence to the optical cavity frequency ν_c. When the laser pulse begins, its frequency is given by

$$\nu = \left(\nu_c\,(1) + \frac{Q_L}{Q_c}\,\nu_L\right) / (1 + Q_L/Q_c) \qquad (5\text{-}11)$$

where subscripts C and L refer to the optical cavity and the CO_2 line, respectively, and Q is the quality factor of the respective resonance. Thereafter, the stimulated emission is in phase with the stimulating radiation, the frequency of which is being swept continuously as a result of the almost adiabatic change in mode volume produced by the moving mirror. During the whole pulse, the frequency probably remains governed by the formula above. Therefore, it is essential to have $Q_L/Q_C \ll 1$. For our cavity, which has a length of 150 cm and power coupling η equal to 0.21 (due to a sodium chloride flat tilted for 20° angle of incidence), we estimate that Q_C is about 8.6×10^6 (neglecting internal losses). Assuming a 60 Mc line width for CO_2, we have a Q_L of about 5×10^5, so that

$$Q_L/Q_C \doteq 0.06. \qquad (5\text{-}12)$$

We have observed a frequency sweep of about 60 Mc in our pulses. Using a Michelson interferometer arrangement with a path length difference of 35 meters, we beat the pulse against itself and observed a 7 Mc signal. The results are shown in Fig. 17, which shows the detector response to the pulse (a) from one arm of the Michelson interferometer and (b) from both simultaneously. This technique will be developed further.

The experiments on SF_6 will be of two kinds, viz., the response of the SF_6 medium to the optical chirps, and the effect of the medium on the pulse propagation. Patel and Slusher (Ref. 45) have used the coincidence of the SF_6 and CO_2 lines to study self-induced transparency. It is probable that the CO_2 line lies in one Doppler wing of the SF_6 absorption and that the SF_6 matrix element is much larger than the reported value (Ref. 45) of 3×10^{-20} esu. The pulse will then select for inversion those SF_6 molecules that fall into a certain velocity component range.

We do not expect to observe self-induced transparency, because of the frequency sweep in our pulses. We hope to observe stimulated emission from the SF_6 following its inversion, and we aim to look for asymmetries in the pulse propagation speed and self-focusing or defocusing effects with respect to the magnitude and sign of

the frequency sweep. The Michelson interferometer scheme may be useful in measuring time delay and phase distortion of the propagating pulse. Focusing and defocusing effects will be studied by observation of diffraction patterns.

Some initial experiments have been conducted to detect the adiabatic inversion of a vibration-rotation transition of sulphur hexafluoride between the ground and first excited states of the ν_3 vibration mode. Using a 12 foot long absorption cell for the SF_6 at a pressure of 7×10^{-3} torr we expect an energy exchange of about 5×10^{-6} joule between the pulse and the medium. Up to the present time this effect has been masked by random fluctuations an order of magnitude greater than this in the energy of the detected pulses. Attempts are being made to eliminate the cause of the fluctuations.

5.3 Future Experiments

The United Aircraft Research Laboratories are engaged in an additional program concerning the investigation of ultrashort laser pulses and their interaction with matter*. Part of this program includes a theoretical and experimental analysis of the detailed substructure of the pulses produced by mode-locked lasers. It has been known for some time that the time-bandwidth product for a pulse from a mode-locked Nd:glass laser is far in excess of the theoretical minimum of unity. This indicates that there is an amplitude or phase substructure to the laser pulse. It was hypothesized that the substructure could have the form of a frequency sweep during the time of a pulse. Such a phase variation could arise from the dispersion within the laser or from nonlinear mechanisms that couple the amplitude and phase of the optical pulse circulating in the laser cavity.

To test this hypothesis an apparatus was constructed that is capable of compensating for a linear chirp and compressing the pulse. It was found that a chirp did exist in the pulse with the optical carrier frequency increasing from the beginning to the end of the pulse. After passing through the apparatus the pulses were compressed from a duration of approximately 4 picoseconds to less than one picosecond.

The apparatus that was used to compress the pulse and measure the duration is shown in Fig. 18. It consists of two plane diffraction gratings arranged so that an incident beam is diffracted from the first grating. The different wavelength components travel at slightly different angles and strike the second grating. The different components are then diffracted again into a direction parallel to their

* The results reported in the first paragraphs of this section were supported by but do not necessarily constitute the opinion of the Air Force Cambridge Research Laboratories, Office of Aerospace Research, under Contract No. F1962867C0075. They are included here because of their intrinsic interest and possible direct application to the subject contract.

original direction. The net result is that the longer wavelengths (lower frequencies) have a longer transit time through the apparatus than the shorter wavelengths (higher frequencies). The transit time is an approximately linear function of wavelength. The difference in transit times for two different wavelengths may be adjusted by changing the grating spacing.

It is evident, then, that such an apparatus can be used to compress a pulse having a positive frequency sweep or to introduce a negative sweep on an originally unswept pulse.

The discovery of the sweep in the pulses produced by a mode-locked Nd:glass laser and the development of the apparatus for introducing a negative sweep lead to the possibility of using ultrashort pulses for adiabatic rapid passage experiments. Efforts will be made to determine the feasibility of such experiments.

Note added in proof: Using the pulse compression technique, it has recently been possible to generate a pulse of 4×10^{-13} seconds duration.

Section 6

OPTICAL RECTIFICATION OF MODE-LOCKED LASER PULSES

The optical rectification (i.e., the nonlinear optical dc polarization) effect was first observed by Bass, et al, in the form of an induced dc voltage across a crystal of potassium dihydrogen phosphate (KDP) during the passage of an intense ruby laser pulse through the crystal[46]. Considerable difficulty is normally encountered in experimentally observing optical rectification because of the low voltage signals generated by the effect, the requirement of relatively broad band and thus insensitive electronic equipment, electrical noise arising from the flash lamp trigger and discharge, and spurious signals due to pyroelectric[46] and acoustic waves generated by the optical electrostriction and transient heating effects[47].

Observations have been made of harmonically-rich electrical pulses generated in crystals of lithium niobate and KDP by the optical rectification of the output of a simultaneously Q-switched and mode-locked Nd:glass laser[48]. The periodic pulsating characteristics of such lasers enabled us to make use of the high sensitivity and selectivity of radio receivers in detecting the effect. The large signal-to-noise ratio obtained by use of a mode-locked laser and a radio receiver in the experiments enabled us to easily identify (and thus eliminate) spurious acoustic signals by their repetitive echo characteristics. In addition, signals from relatively slow effects such as the pyroelectric effect were eliminated by detecting the harmonics of the optical rectification signals in the microwave region.

The output of the mode-locked Nd:glass laser used in our experiments consisted of a series of light pulses of 10^{-12} to 10^{-11} sec time duration[48,49,50], evenly spaced by the optical transit time of the laser cavity. The fundamental frequency of the pulse train used here was 275 MHz. The average energy in the individual pulses was typically of the order of 1 mJ. The entire pulse train contained approximately 200 pulses and lasted about 0.6 μsec. The laser output was directed through crystals of lithium niobate and KDP either along or perpendicular to the z-axis of the crystals. A flat-ended coaxial probe fixed against the surface normal to the z-axis was used to sense the induced fields present at that surface. A 5-mil-thick annular mylar gasket was used to prevent an intimate contact between the center probe and the crystal surface to eliminate the possible acoustic effects[47] which might cause spurious signals through the surface piezoelectric effect, especially in the case of lithium niobate. Such acoustic signals could be identified by their repetitive echo characteristics. The rf signals were measured to be approximately 2 mv and were detected by a superheterodyne receiver having a 20 MHz bandwidth.

The observed signals were recorded with a signal-to-noise ratio of up to 20 to 25 db and followed the general features of the envelope of the laser pulse train which was simultaneously recorded. Signals were recorded at each harmonic frequency

from 275 MHz to 9.025 GHz and were limited only by the available equipment. As evidenced by tuning the radio receiver, the signals were as well confined to the harmonic frequencies of the laser pulse repetition frequency as the bandwidth of the receiver could determine. The actual bandwidth of the observed signals can be calculated from the length of the entire pulse train. In the case of lithium niobate, the phase matching angle for efficient second harmonic light production is very nearly normal to the optic axis so it was possible to simultaneously observe the optical rectification signal, the second harmonic (green) light output and the original input laser pulse train.

Figure 19 schematically illustrates the orientation of the crystallographic axes of KDP with respect to the polarization of the repetitive pulses. For KDP illuminated along the z-axis, the dc part of the polarization reduces simply to $P_z = 1/2 X_{zxy} E_x E_y$, where $_{zxy}$ is the third rank nonlinear dielectric tensor for KDP. If θ is the angle between the plane of polarization of the laser light and the x-axis of the KDP, P_z will vary as sin 2θ. Figure 20 shows the relative strength of the rf signals at 2.75 GHz recorded as a function of θ. The sin 2θ function has been normalized and drawn as the dashed curve for comparison. Similar data were observed at other harmonic frequencies. Signals from relatively slow effects, such as the pyroelectric effect, were eliminated by detecting the optical rectification effect at microwave frequencies. Figure 21 illustrates typical oscillograms of the optical rectification and laser output signals.

The broad band response of the optical rectification effect, coupled with greatly increased sensitivity obtained with radio receivers and repetitive picosecond laser pulses, suggests the use of the effect for detecting picosecond light pulses and for generating millimeter and submillimeter radiation. Optical pulse measurement by the optical rectification effect is similar to pulse intensity correlation measurements[49-51]. The correlation measurements reported in the past were performed in the Fourier transform or frequency domain. Some unique characteristics of such a microwave generating system would be its broad band passive generating element (i.e., the nonlinear crystal) whose operating frequencies can be easily changed and precisely specified by adjustment of the laser cavity length. The upper operating frequency of the device is limited only by the harmonic content of the available ultrashort laser pulses.

Section 7

MODE-LOCKING OF AN ORGANIC DYE LASER

7.1 Introduction

It has been reported that a large number of organic dye solutions exhibit laser action when excited with a short duration, high-intensity pump pulse (Refs. 52-56). Pump pulses from Q-switched lasers and from specially constructed flash tubes have been employed. The output spectra from such dye lasers are quite broad, extending in some cases over a few hundred angstroms. This suggests the possibility of mode-locking an organic dye laser to produce very short (picosecond or shorter) pulses over a wide range of the visible spectrum. The availability of ultrashort pulses with any desired wavelength would greatly increase their applicability to studies of nonlinear transient optical effects, spectroscopy, and lifetime measurements (Ref. 48).

Mode-locking of a laser-pumped dye laser has been achieved. A flashlamp pumped dye laser has also been constructed, and efforts will be made to mode-lock it with a saturable absorber. In addition, it may be possible to use the flashlamp pumped laser to perform experiments on two-photon gain. This possibility is discussed in Section 7.4.

7.2 Mode-locking of a Laser-Pumped Laser

It is well known that a periodic modulation of the gain of a laser medium will lead to mode-locking if the frequency of the modulation is equal to or a multiple of the difference frequency between longitudinal modes of the laser. If the pumping signal for a dye laser consists of a mode-locked train of pulses, the gain of the laser will have a periodic variation with a period equal to the spacing between the pumping pulses. If the length of the dye laser cavity is equal to or a submultiple of the length of the cavity of the laser producing the pump pulses, then the mode-locking condition will be satisfied and the output of the dye laser will consist of a series of pulses.

Rhodamine 6G and Rhodamine B in ethanol solution have absorption peaks at 5260 Å and 5500 Å respectively. These peaks are sufficiently broad to allow efficient pumping with the 5300 Å second harmonic of the Nd:glass laser. These dyes were used as the lasing media in the experiments to be described.

Several different configurations have been successfully operated. The first configuration that was used is illustrated in Fig. 22. The dye cell was 2.5 cm in diameter and 5 cm in length. The windows were optically flat and positioned almost perpendicular to the axis of the cell. The mirrors had a 1-meter radius of curvature and a reflectivity in excess of 90% between 5000 Å and 6000 Å. The second harmonic required for pumping was generated in the dye cavity with a crystal of phase-matched KDP. The efficiency of conversion of the 1.06 micron radiation to

second harmonic was measured to be approximately 2%. A slight focusing of the fundamental radiation into the dye laser cavity was required to reach threshold.

The strength of the dye solution was adjusted by gradually increasing the dye concentration until the second harmonic radiation was almost completely absorbed in the cell. Typical concentrations used were about 10^{-4} molar.

The pump signal was generated as the second harmonic from a Nd:glass laser that was mode-locked with Eastman Kodak 9740 dye[48, 57]. The length of the rod was 6" and the diameter 0.5". The output consisted of a train of subnanosecond pulses spaced by approximately 5×10^{-9} sec and lasted approximately 2×10^{-7} sec.

Lasing was observed with the optical length of the dye laser cavity equal to 1, 1/2 and 1/3 times the length of the pumping laser cavity. Figure 23a shows a typical output of the pumping laser. Figure 23b shows a synchronous trace of the dye laser output. In this case the dye laser cavity was adjusted to be one-half of the length of the pumping laser cavity. The dye used in this case was Rhodamine 6G in ethanol. The dye laser output shows very small fluorescence until the pumping signal reaches threshold, at which point the dye laser breaks into oscillation and produces a series of pulses at twice the repetition rate of the pumping pulses. The energy scale on the traces is intended to give a rough estimate of the pulse energies. The vertical axis is given in energy rather than power because the fundamental pulses are shorter than the response time of the detector. The pulse shape is thus characteristic of the detector rather than any property of the pulse. The only quantity that can be measured is the total energy of the pulse, which is proportional to the amplitude of the detector-limited pulse shape. The same procedure was used for the dye laser output, with appropriate scaling of the spectral sensitivities of the two diodes. These values are somewhat uncertain, therefore, since the pulse duration is comparable to the detector response time.

Figures 23c, 23d show the spectral output of the dye laser and a mercury reference spectrum. Figure 23c shows the output for a 5×10^{-5} molar solution of Rhodamine B in ethanol. The output occurs slightly above the 5790 Å line of the mercury spectrum. For Rhodamine 6G of comparable concentration, the line appears midway between the two mercury lines, at 5600 Å. If Rhodamine 6G is added to the Rhodamine B solution, the line moves continuously from one limit to the other. Such an intermediate case is shown in Fig. 23d.

It was noted that the spectral width of the output of this laser was not as great as has been reported.[28] It was felt that this was due to the fact that the laser was operating just above threshold. The output pulses from this laser were longer than those of the pump and were comparable to the response time of the detector.

To achieve higher pumping, the laser was redesigned. The broad band mirrors were replaced with dielectric reflectors with a very sharp cut on of the reflectivity. The reflectivity of the mirrors was less than 20% at 5300 Å and rose

sharply to greater than 90% from 5500 Å to 7000 Å. This characteristic made it possible to generate the second harmonic radiation outside the dye laser cavity. A crystal of KDP of better optical quality was used and the second harmonic radiation was passed through a telescope to reduce the beam diameter by a factor of approximately 3. The dye cell, similar to that described above, was filled with a solution of Rhodamine 6G in ethanol having an optical density of 1.0 cm^{-1} at 5300 Å.

The behavior of this laser as a function of the cavity length is shown in Fig. 24. In this series of experiments the optical length of the pumping laser cavity was 34". Mode-locking should occur when the length of the dye laser cavity is made equal to one-half (or equal to) the pumping laser cavity. At a length of 19", partial mode-locking was observed. The depth of modulation increased as the cavity length was decreased until complete modulation was observed at 17".

Figure 25a illustrates the output of the laser on an expanded time scale. It should be noted that the pulse width is now less than the response time of the detection system as evidenced by the slight undershoot of the waveform on the oscilloscope. The modulation on the envelope is due to the fact that a pumping pulse is present only for every second dye laser pulse.

Figure 25b illustrates the spectral output of the laser. The output for this laser was centered at 5660 Å and had a width of more than 100 Å.

The pulses produced by this laser were certainly less than one nanosecond in length. Future work will be directed toward measurement of the actual duration using the two photon absorption-fluorescence technique.

7.3 Flashlamp Pumped Dye Laser

A high-speed coaxial flashlamp-dye cell similar in design to that of Sorokin et al.[58] has been constructed (see Fig. 26) and tested. The arc length in the discharge region is about 13 cm long. The liquid cell is about 21 cm long. Both the gas (air) in the discharge region and the liquid in the cell are continuously flowed. The capacitor bank used with the flashlamp consists of two series connected Maxwell Laboratories 12ED-6LN capacitors. These are attached directly to the flashtube using the tabs shown in Fig. 26. The bank has a total energy storage of 86 joules at the rated voltage of 24 kV.

To fire the lamp the leakage rates of air into and out of the discharge region are adjusted to between 1 and 100 mm pressure. The capacitors are then charged until the air breaks down. The flash produced has a rise time of about 0.3 s and a half width of slightly under 1 μsec. With a broadband 100% reflector at one end, a cavity and an 80% reflector at the other, it was found possible to produce lasing in a 2×10^{-4} M. ethanol solution of fluorescein sodium and in a 5×10^{-4} M. ethanol solution of Rhodamine 6G. These are the only two solutions tried to date. No definitive energy or pulse duration measurements have yet been made.

With his device Sorokin has obtained outputs of 0.2 joules in pulses with a peak power of about 0.5 Mw from Rhodamine 6G. By increasing the pump power it should be possible to increase this output considerably. An Mg_2O reflector on the outside of the flashlamp should also prove useful for this purpose. Such intensities would be adequate for studying non-linear optical effects in the visible and near UV region. Because of the proximity of the ultraviolet electronic resonances, such effects could be very large.

Very recently a flashlamp pumped Rhodamine 6G dye laser was mode-locked using a saturable absorber. It should be possible to find saturable absorbers for nearly all the dye lasers. Indeed, most of the more common polymethine cyanine dyes have their principal absorptions in the visible region. (The dyes used for mode-locking the neodymium laser, the ruby laser and the Rhodamine 6G dye laser). Efforts will be made to find suitable dyes to mode-lock a variety of organic dye lasers.

7.4 Two-Quantum Gain Experiment

It has recently been pointed out by V. S. Letokov[60] that it should be possible to obtain a nonlinear gain characteristic by stimulating two-quantum emission in an inverted medium. Such a process would give, under certain conditions, a gain that is proportional to the pulse intensity. This would result in dramatic sharpening of the pulse envelope.

It was also suggested in the above reference that organic dye lasers might provide a suitable medium for experimentation, with the nonlinear gain medium placed inside or outside the laser cavity.

Efforts will be made to determine the feasibility of such experiments using either the flash lamp pumped dye laser or a laser pumped dye laser to sharpen the pulses from mode-locked ruby or Nd:glass lasers.

Section 8

TWELVE MONTH STATUS EVALUATION

8.1 Summary of Results

This report presents a summary of the research performed by the United Aircraft Research Laboratories during the twelve-month interval from 1 August 1967 to 31 July 1968 on problems concerned with advancing the state of the art of ultrashort laser pulse technology. The effort has resulted in the following accomplishments:

(a) Analysis of the Propagation of Ultrashort Optical Pulses. A description is given of a theoretical model which accounts for certain novel effects that take place when extremely short pulses of coherent light interact with matter. It is shown that the interaction of an assembly of two-level systems with a light pulse having a duration that is short compared to all relaxation times of these systems can be described in terms of a single nonlinear partial differential equation. The equation is one which also occurs in differential geometry. Techniques available for obtaining particular solutions of this equation may be employed to derive analytical expressions which describe the observed breakup of short pulses as well as the self-induced transparency effect. Analytical solutions describing the propagation of 2π and 4π pulses have been derived and could be generalized to describe the behavior of $2n\pi$ pulses.

(b) Measurement of Nanosecond Fluorescence Decay Time. This accomplishment has demonstrated how ultrashort laser pulses of high peak power may be used to measure nanosecond fluorescent lifetimes. The techniques can be extended to the measurement of subnanosecond decay times.

(c) Light Amplification in Saturable Absorbers (LAISA) with Picosecond Pulses. It has been found that an absorber, driven into saturation by an intense light pulse from a mode-locked ruby laser, can amplify a weaker light pulse simultaneously incident upon the medium. Energy gains as high as 20 times have been observed in a 1 cm path length in the saturable absorber solution. A theory giving qualitative agreement with the experimental results has been developed. The effect has an important bearing on the subject of mode-locking with saturable absorbers.

(d) Adiabatic Inversion of Quantum States. A theoretical investigation of the interaction of an intense, frequency-swept pulse of light (i.e., an optical chirp) with matter has been conducted. The first interesting result to come out of the investigation was the adiabatic inversion of populations between a pair of levels when the frequency of the pulse is swept through their resonant frequency. The second result was the dependence of the phase of the induced polarization on the direction of the sweep. An experiment to attempt to observe these effects is in progress. In connection with this experiment a 60 MHz frequency swept, Q-switched CO_2 laser has been developed. This should also have application to problems in optical ranging and signal processing.

(e) Optical Rectification of Mode-Locked Laser Pulses at Microwave Frequencies. This accomplishment opens up the possibility of generating millimeter or submillimeter waves with ultrashort optical pulses and obtaining a detector for picosecond pulses because of the broad band response of the optical rectification effect. The detection of optical rectification at approximately 10 GHz has eliminated spurious signals from pyroelectric and acoustic effects, therefore simplifying the detection of this effect. The use of simultaneously Q-switched and mode-locked pulses enables the use of the high sensitivity characteristics of radio receivers in many experiments where signal sensitivity may be a problem.

(f) Mode-locking of Organic Dye Lasers. A laser-pumped organic dye laser has been developed and has resulted in the production of subnanosecond (possibly picosecond) pulses at the dye laser wavelength. Further work in this area should make available picosecond optical pulses throughout the visible portion of the spectrum. The availability of ultrashort pulses at any desired wavelength would greatly increase their applicability to studies of nonlinear optical effects, lifetime measurements, etc. Work has also been conducted on flashlamp pumped dye lasers and such lasers have been successfully operated. It is anticipated that this type of laser will be useful for mode-locking and other experiments involving nonlinear gain processes.

8.2 Publications and Presentations

The following is a list of publications and presentations for which partial or complete support can be attributed to the present contract. The order generally follows the order of presentation of results in this report, with general reviews grouped at the end.

1. G. L. Lamb, Jr., "Propagation of Ultrashort Optical Pulses," Phys. Letters 25A, 181 (1967).

2. G. L. Lamb, Jr., Lecture at Summer School in Quantum Electronics held at Flagstaff, Arizona, June 17-28, 1968.

3. G. L. Lamb, Jr., "Propagation of Ultrashort Optical Pulses," to be published in Festschrift for P. M. Morse, Technology Press, M.I.T.

4. M. E. Mack, "Measurement of Nanosecond Fluorescent Decay Lines," J. Appl. Physics 39, 2483 (1968).

5. M. E. Mack, "Light Amplification in Saturable Absorbers," Appl. Phys. Letters 12, 329 (May 15, 1968).

6. M. E. Mack, "Optical Gain in Saturable Absorbers," accepted for publication in in the IEEE Journal of Quantum Electronics.

7. M. E. Mack, "Recovery Time and Non-Linearities in Bleachable Absorbers," presented at the 1968 International Quantum Electronics Conference, Miami, Florida (May 14-17, 1968).

8. M. E. Mack, "Light Amplification in Saturable Absorbers," presented as a post deadline paper at the 1968 International Quantum Electronics Conference, Miami, Florida (May 14-17, 1968).

9. E. B. Treacy, "Generation of Chirped Pulses at 10.6 Microns Wavelength," to be published in Proceedings of the IEEE.

10. E. B. Treacy, "Adiabatic Inversion with Light Pulses," to be published in Phys. Letters.

11. M. J. Brienza, A. J. DeMaria, and W. H. Glenn, "Optical Rectification of Mode-Locked Laser Pulses," Phys. Letters 26A, 390 (1968).

12. M. J. Brienza, A. J. DeMaria and W. H. Glenn, "Optical Rectification of Mode-Locked Laser Pulses" presented at the 1968 International Quantum Electronics Conference, Miami, Florida (May 14-17, 1968).

13. W. H. Glenn, M. J. Brienza, A. J. DeMaria, "Mode-Locking of an Organic Dye Laser," Appl. Phys. Letters 12, 54 (1968).

14. A. J. DeMaria, "Nonlinear Optical Studies with Picosecond Light Pulses," (Invited) A.P.S. March Meeting in Berkeley (March 18-21, 1968).

15. A. J. DeMaria, "Nonlinear Interaction of Subnanosecond Light Pulses," (Invited) Optical Society of America, Washington, D.C. (March 13-16, 1968).

16. W. H. Glenn, "Generation and Measurement of Picosecond Pulses," (Invited) A.P.S. February Meeting in Boston (Feb. 26-28, 1968).

17. A. J. DeMaria, "Picosecond Laser Pulses," E.E. Seminar, Ohio State University (March 1968).

18. A. J. DeMaria, "Generation Measurement and Utilization of Picosecond Laser Pulses," (Invited) M.I.T. Lincoln Laboratory (Feb. 14, 1968).

19. A. J. DeMaria, "Picosecond Laser Pulses," Physics Seminar, Bell Telephone Laboratories, Holmdel, N.J. (January 1968).

20. W. H. Glenn, "Generation and Measurement of Properties of Picosecond Laser Pulses," (Invited) Fall 1967 URSI and IEEE G-AP Meetings (October 16-19, 1967).

21. A. J. DeMaria, "Ultrashort Light Pulses," (Invited) NEREM, Boston, Massachusetts (October, 1967).

22. A. J. DeMaria, Lecture at Summer School in Quantum Electronics held at Flagstaff, Arizona (June 17-28, 1968).

23. M. E. Mack, "Measurement of Nanosecond Fluorescent Decay Times," Conference on Subnanosecond Light Pulses, Durham, North Carolina (November 14-17, 1967).

REFERENCES

1. A.J. DeMaria, D.A. Stetser and W.H.Glenn, Jr., Science 156, 1557 (1967); G. Magyar, Nature 218, 16 (1968). Both of these survey articles contain extensive reference to the original research publications.

2. R. Bellman, G. Birnbaum and W.G. Wagner, J. Appl. Phys. 34, 750 (1963); L.M. Frantz and J.S. Nodvik, J. Appl. Phys. 34, 2346 (1963); J.P. Wittke and P.J. Warter, J. Appl. Phys. 35, 1668 (1964).

3. C.L. Tang and B.D. Silverman, in Physics of Quantum Electronics, edited by P.L. Kelley, B. Lax and P.E. Tannenwald (McGraw-Hill Book Co., Inc., New York, 1966) p. 280. Although this paper is not addressed to short-pulse propagation, the formalism is adequate for such considerations.

4. S.L. McCall and E.L. Hahn, Phys. Rev. Letters 18, 908 (1967).

5. F. Hopf and M.O. Scully, to be published.

6. C.K.N. Patel and R.E. Slusher, Phys. Rev. Letters 19, 1019 (1967).

7. F. Bloch, Phys. Rev. 70, 460 (1964).

8. W.E. Lamb, Jr., in Proceedings of the International School of Physics "Enrico Fermi," Course XXXI, edited by P.A. Miles (Academic Press, Inc., New York, 1964), Phys. Rev. 134, A1429 (1964).

9. N.G. Basov, et al., Soviet Physics JETP 23, 16 (1966).

10. Private communication from M.O. Scully of M.I.T.

11. L.P. Eisenhart, A Treatise on the Differential Geometry of Curves and Surfaces (Dover, New York, 1960), p. 23.

12. Ref. 11, p. 25.

13. The author is indebted to E.B. Treacy for this observation.

14. The relevance of this equation to optical pulse propagation was apparently first discovered by C. Cercignagni and A. Chirardi and is referred to by F.T. Arecchi and R. Bonifacio, IEEE J. Quant. Electr. 1, 169 (1965) where a summary of their calculation is presented. Discussion of this equation in relation to other physical problems of contemporary interest may be found in A. Seeger, et al., Z. Physik 134, 173 (1953); P. Lebwohl and M.J. Stephen, Phys. Rev. 163, 376 (1967).

15. Ref. 11, p. 280 et seq.

16. A.R. Forsyth, Theory of Differential Equations (Dover, New York, 1959), Vol. VI, Chap. 21. Additional references are cited herein. M.J. Clairin, Annales de Toulouse 2e Sér. 5, 437 (1903).

17. Ref. 11, p. 286.

18. G.L. Lamb, Jr., Phys. Lett. 25A, 181 (1967). In this work the analysis was improperly applied to the amplifier case .

19. C.K.N. Patel and R.E. Slusher (to be published).

20. P.M. Morse and H. Feshbach, Methods of Theoretical Physics (McGraw-Hill Book Co., Inc., New York, 1953), Vol. I, pp. 734 and 768 and Vol. II, p. 1651.

21. Ref. 11, p. 284.

22. W. Szymanowski, Z. f. Phys. 95, 450 (1953); P. Pringsheim, Fluorescence and Phosphorescence, pp. 10-17, Interscience Publishers, New York, (1949).

23. H.W. Mocker and R.J. Collins, Appl. Phys. Letters 7, 270 (1965).

24. M. H. Crowell, IEEE (Inst. Elec. Electron. Engrs.) J. Quantum Electron. 1, 12 (1965).

25. M. DiDomenico, J.E. Geusic, H.M. Marcos and R.G. Smith, Appl. Phys. Letters 8, 180 (1966).

26. M.B. Fisher and R.T. McKenzie, International Electron Devices Meeting, Washington, D. C., October 1967.

27. R.J. Carbone and P.R. Longaker, Appl. Phys. Letters 4, 32 (1964).

28. P.P. Sorokin, J.R. Larkard, E.C. Hammond and V.L. Morruzi, IBM Journal, 11, 130 (1967).

29. P.P. Sorokin and J.R. Lankard, IBM Journal 11, 148 (1967).

30. M.L. Spaeth and W.R. Sooy, 4th International Conference on Quantum Electronics (1966).

31. P.W.A. Bowe, W.E.K. Gibbs and J. Tregellas-Williams, Nature 209, 65 (1966).

32. F.T. Arecchi, V. Degiorgio and A. Sona, Nuovo Cimento 38, 1096 (1965).

33. B. Senitzky, G. Gould and S. Cutler, "Millimeter-Wave Amplification by Resonance Saturation", Phys. Rev., 130, 1460-1465 (1963).

34. S.E. Schwartz and T.Y. Tan, "Wave Interactions in Saturable Absorbers", Appl. Phys. Letters, 10, 4-7 (1967).

35. B.H. Soffer and B.B. McFarland, "Frequency Locking and Dye Spectral Hole Burning in Q-Spoiled Lasers," Appl. Phys. Letters, 8, 166-169 (1966).

36. M.L. Spaeth and W.R. Sooy, "Experimental Studies of Passive Q-Switched Parameters", Hughes Aircraft Company Report.

37. R.Y. Chiao, P.L. Kelley and E. Garmire, "Stimulated Four-Photon Interaction and its Influence on Stimulated Rayleigh-Wing Scattering", Phys. Rev. Letters 17, 1158-1160 (1966).

38. S.L. McCall and E.L. Hahn, "Self-Induced Transparency by Pulsed Coherent Light", Phys. Rev. Letters 18, 908-911 (1967).

39. M.E. Mack, "Mode-Locking the Ruby Laser", to be published.

40. A. Abragam, The Principles of Nuclear Magnetism, Oxford University Press (1961).

41. I.D. Abella, S.R. Hartmann and N.A. Kurnit, Physical Review 141, 391 (1966).

42. E.L. Hahn, Phys. Rev. 80, 580 (1950).

43. H.Y. Carr and E. M. Purcell, Phys. Rev. 94, 630 (1954)

44. R.P. Feynman, F.L. Vernon and R.W. Hellwarth, J. Appl. Phys. 28, 49 (1957)

45. C.K.N. Patel and R.E. Slusher, Phy. Rev. Letters 19, 1019 (1967).

46. M. Bass, P.A. Franken, J.F. Ward and G. Weinreich, Phys. Rev. Letters, 9, 446 (1962).

47. M.J. Brienza and A.J. DeMaria, Appl. Phys. Letters 11, 44 (1967).

48. A.J. DeMaria, D.A. Stetser and W.H. Glenn, Jr., Science 156, 1557 (1967)

49. W.H. Glenn, Jr., and M.J. Brienza, Appl. Phys. Letters 10, 221 (1967.

50. J.A. Armstrong, Appl. Phys. Letters 10, 16 (1967).

51. J.A. Giordmaine, P.M. Rentzepis, S.L. Shapiro and K.W. Wecht, Appl. Phys. Letters 11, 216 (1967)

52. P.P. Sorokin, J.R. Lankard, E.C. Hammond and V.L. Morruzi, IBM Journal 11, 130 (1967).

53. M. Bass and T.F. Deutsch, Appl. Phys. Letters 11, 89 (1967).

54. B.H. Soffer and B.B. McFarland, Appl. Phys. Letters 10, 226 (1967).

55. M.L. Spaeth and D.P. Bortfeld, Appl. Phys. Letters 9, 179 (1966).

56. F.P. Schaefer, W. Schmidt, J. Volze, Appl. Phys. Letters 8, 306 (1966).

57. A.J. DeMaria, D.A. Stetser and H.A. Heynau, Appl. Phys. Letters 8, 174 (1966).

58. P.P. Sorokin, J.R. Lankard, V.L. Moruzzi and E.C. Hammond, IBM Research Paper RC-1950, "Flashlamp Pumped Organic Dye Lasers," November 30, 1967.

59. W. Schmidt and F. P. Schafer, Phys. Letters 26A, 558 (1968).

60. V. S. Letokov, ZhETF Pisma 7, 284 (1968), JETP 7, 221 (1968).

LIST OF FIGURES

LIST OF FIGURES (Cont'd)

TABLE I - LIQUID LASER DYES

DYE	SOLVENT	FLUORESCENT PEAK	FLUORESCENT LIFETIME
Acridine Red	Ethanol	5800Å	2.4 nsec
Acridine Yellow	Ethanol	5050Å	5.2 nsec
Sodium Fluorescein	Ethanol	5270Å	6.8 nsec
Rhodamine 6G	Ethanol	5550Å	5.5 nsec
Rhodamine 6G	Water	5550Å	5.5 nsec
Acridone	Ethanol	4370Å	11.5 nsec
Anthracene	Methanol	4000Å	4.5 nsec

TABLE II - Q-SWITCHING DYES

DYE	SOLVENT	ABSORPTION PEAK	FLUORESCENCE PEAK	LIFETIME
CAP	Ethanol	6700Å	7750Å	10.1 nsec
CAP	Methanol	6710Å	7550Å	10.3 nsec
CAP	Chloronaphthalene	6970Å	7380Å	8.0 nsec
VP	Nitrobenzene	6980Å	--	4.1 nsec
VP	Chloronaphthalene	7010Å	--	4.2 nsec
CC	Methanol	7060Å	7400Å	0.5 nsec

CAP = Chloro-Aluminum Phthalocyanine

VP = Vanadyl Phthalocyanine

CC = Cryptocyanine

G920479-8

FIG. 1

SCHEMATIC REPRESENTATION FOR THE BAECKLUND TRANSFORMATION GIVEN BY EQUATION (2-37)

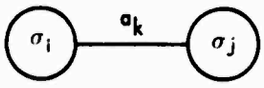

FIG. 2

DIAGRAM FOR SEQUENCE OF TRANSFORMATIONS GIVING 4π PULSE

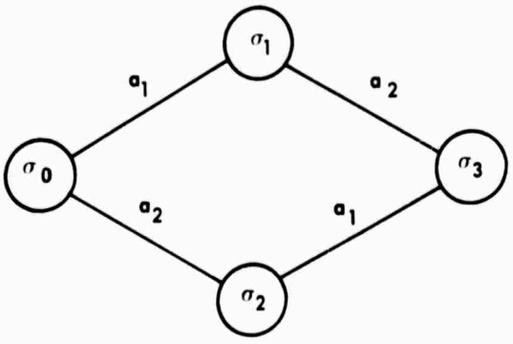

G920479-8

FIG. 3

PROPAGATION OF A 4π PULSE IN AN ABSORBING MEDIUM

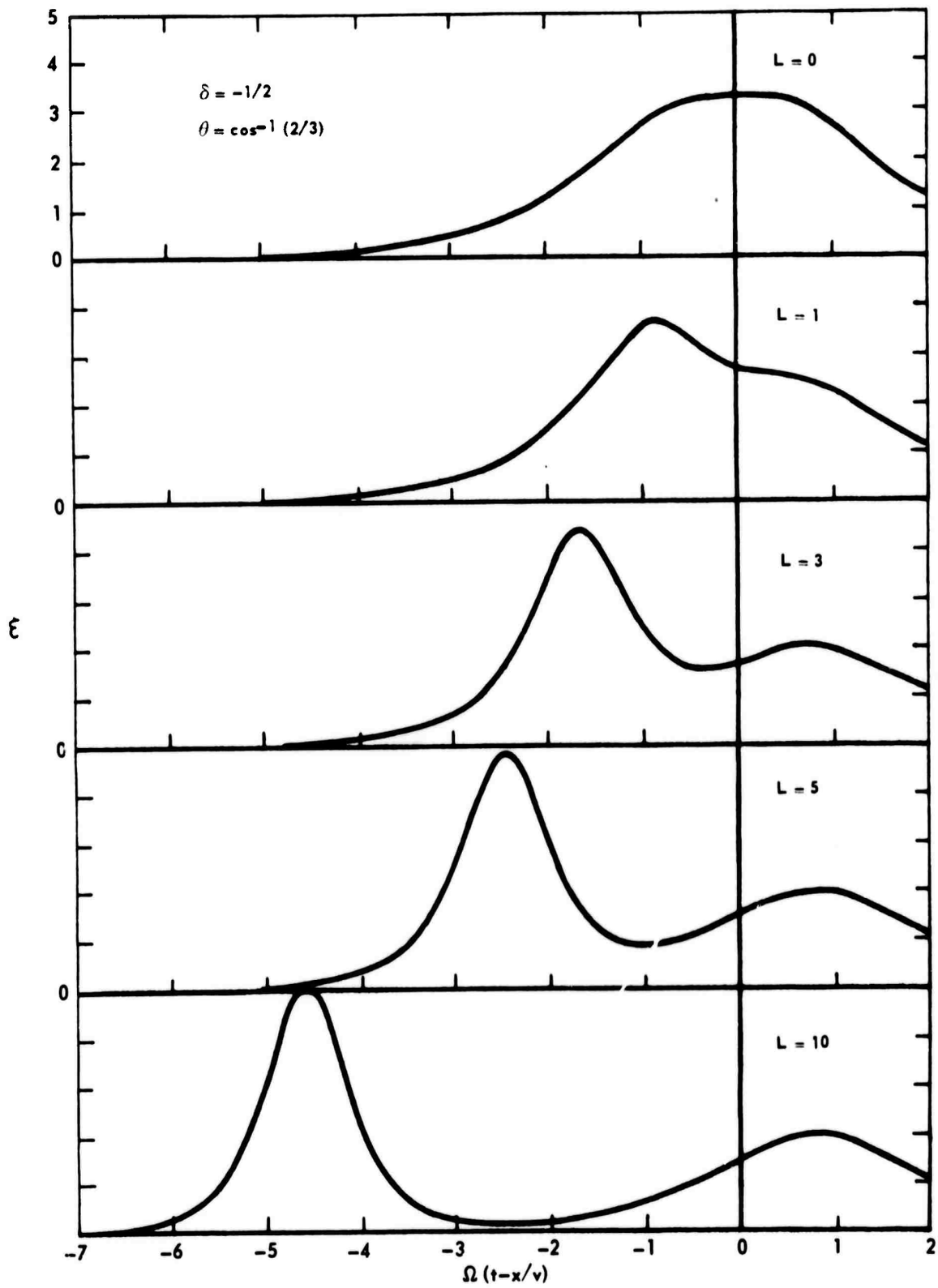

FIG. 4

DIAGRAM FOR SEQUENCE OF TRANSFORMATIONS GIVING 6π PULSE

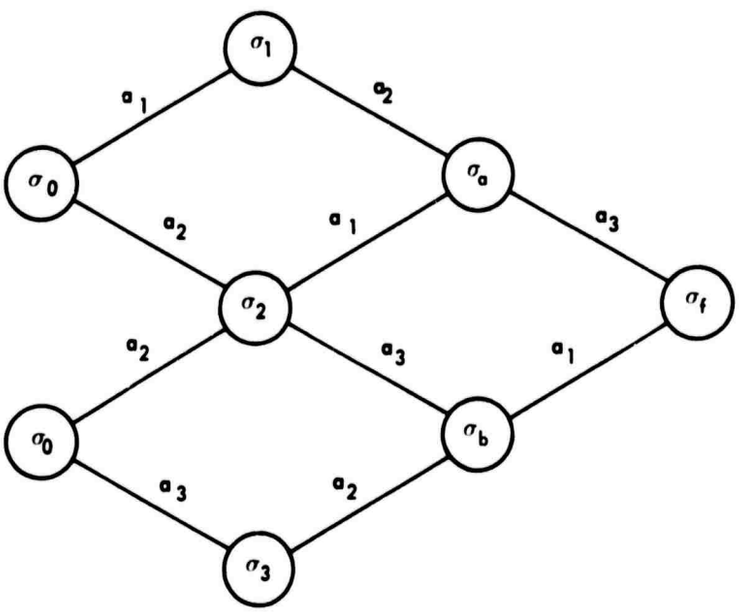

G920479-8

FIG. 5

BREAKUP OF 6π PULSE AS DERIVED FROM SEQUENCE OF TRANSFORMATIONS SHOWN IN FIG. 4

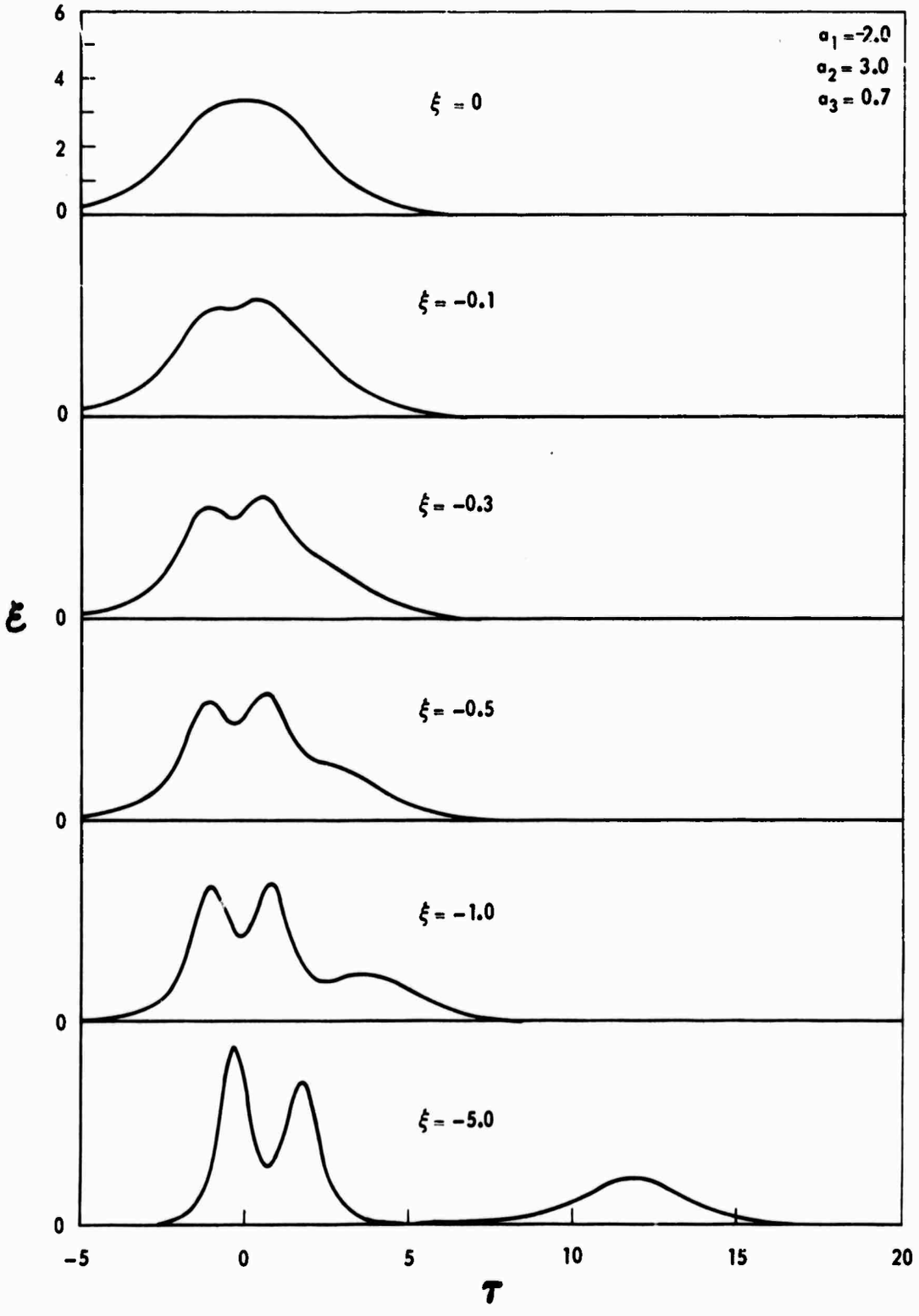

G920479-8

FIG. 6

TYPICAL OSCILLOGRAMS

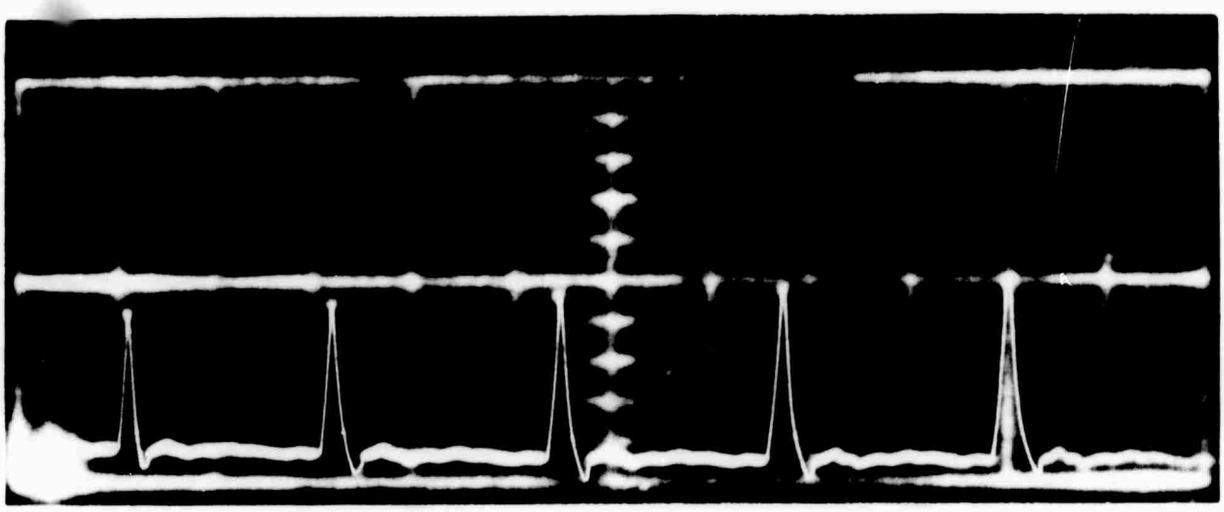

(a) MODE-LOCKED RUBY LASER OUTPUT • 10 nsec/cm

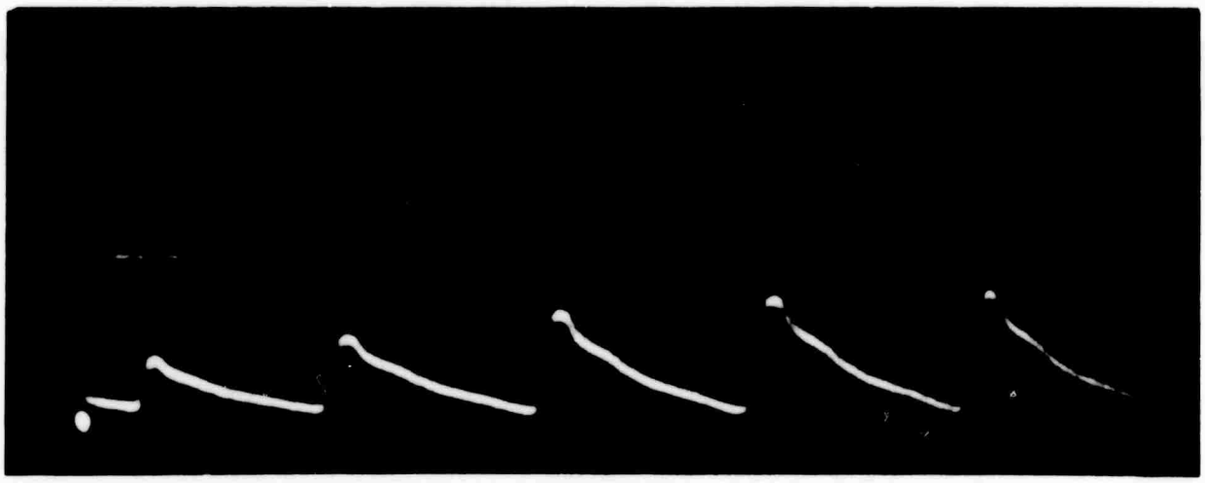

(b) FLUORESCENCE DECAY TIME OF FLUORESCEIN SODIUM • 10 nsec/cm

EXPERIMENTAL ARRANGEMENT USED FOR LIQUID LASER DYE LIFETIME MEASUREMENTS

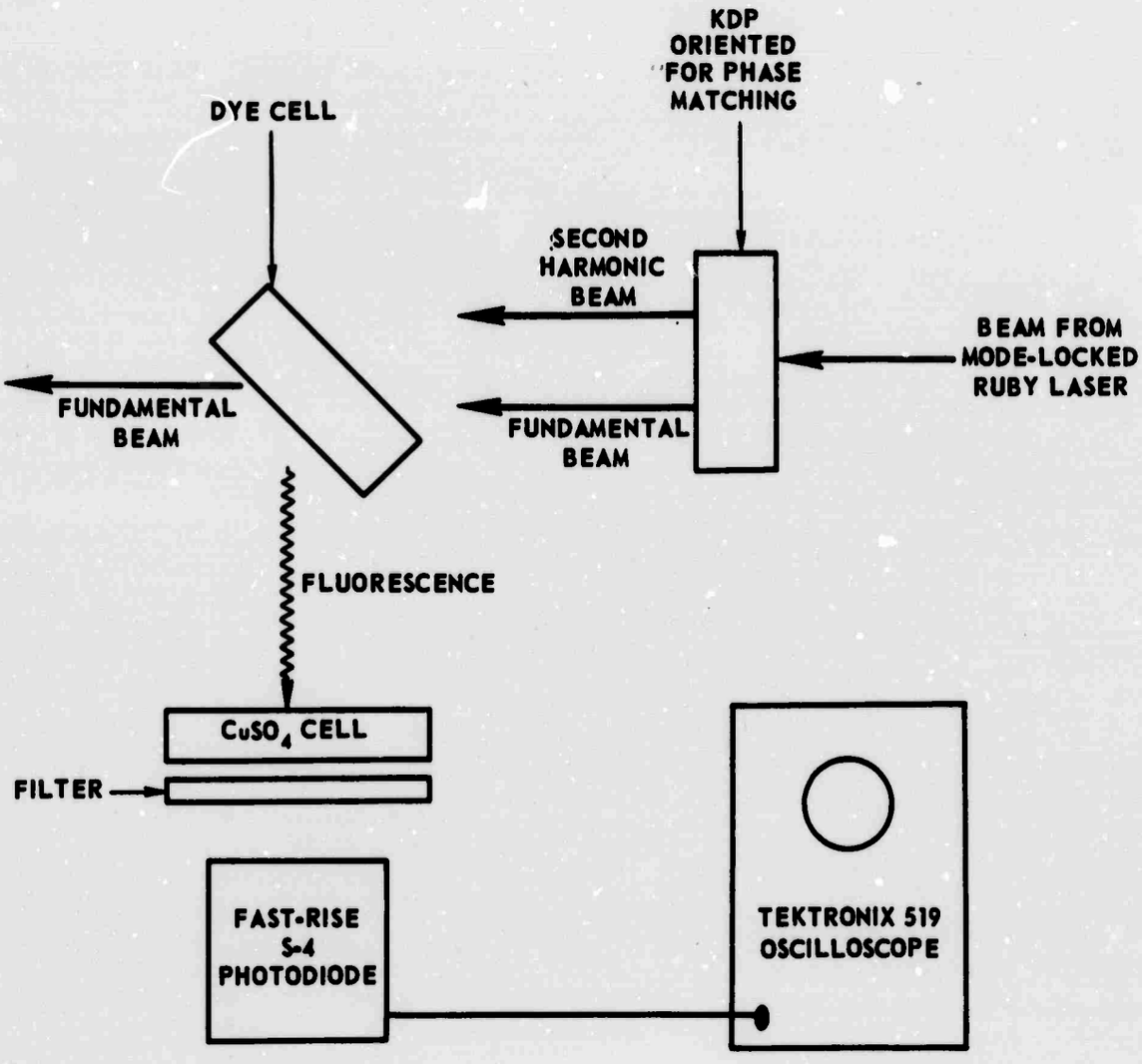

EXPERIMENTAL ARRANGEMENT FOR OBSERVING GAIN IN SATURABLE ABSORBERS

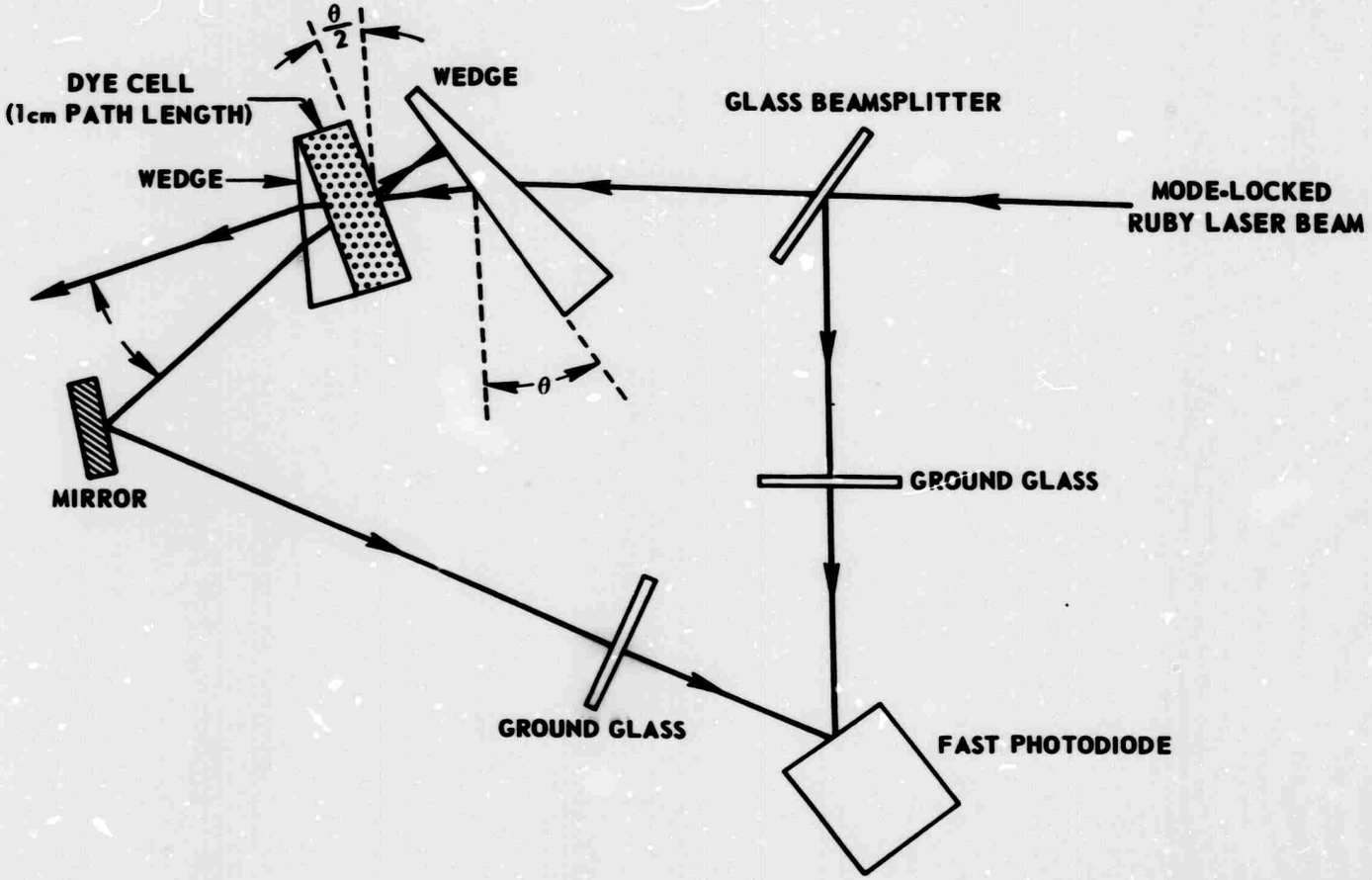

G920479-8

FIG. 8

G920479-8

FIG. 9

EXPERIMENTAL RESULTS ILLUSTRATING GAIN

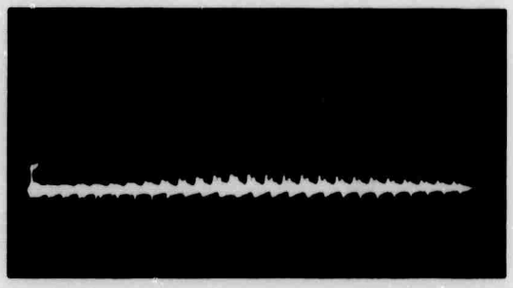

(a)

(b)

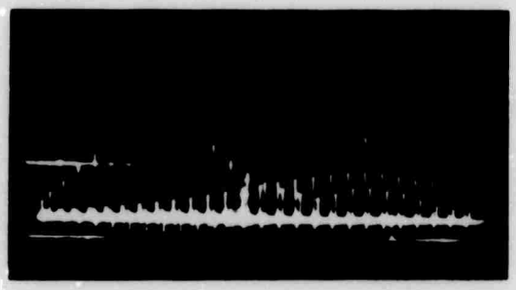

(c)

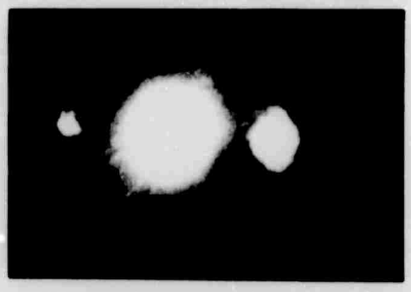

(d)

G920479-8

FIG. 10

ANGULAR DEPENDENCE OF THE GAIN

θ = 25 MRAD

θ = 18 MRAD

θ = 11 MRAD

θ = 7 MRAD

θ = 4 MRAD

G920479-8

FIG. 11

(a) GENERATED WAVE INTENSITY

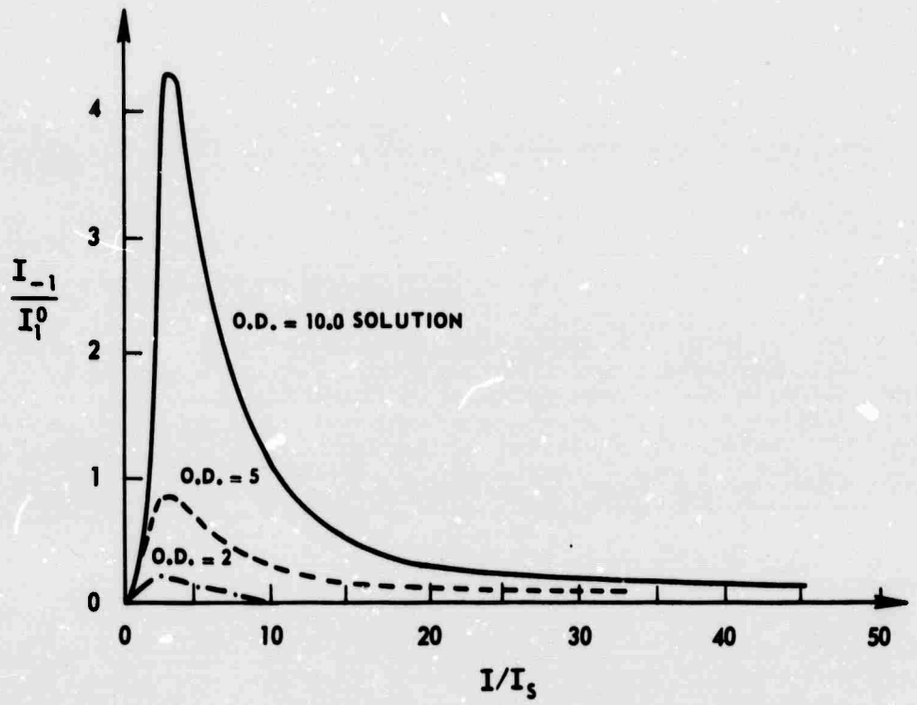

(b) PROBING WAVE POWER GAIN

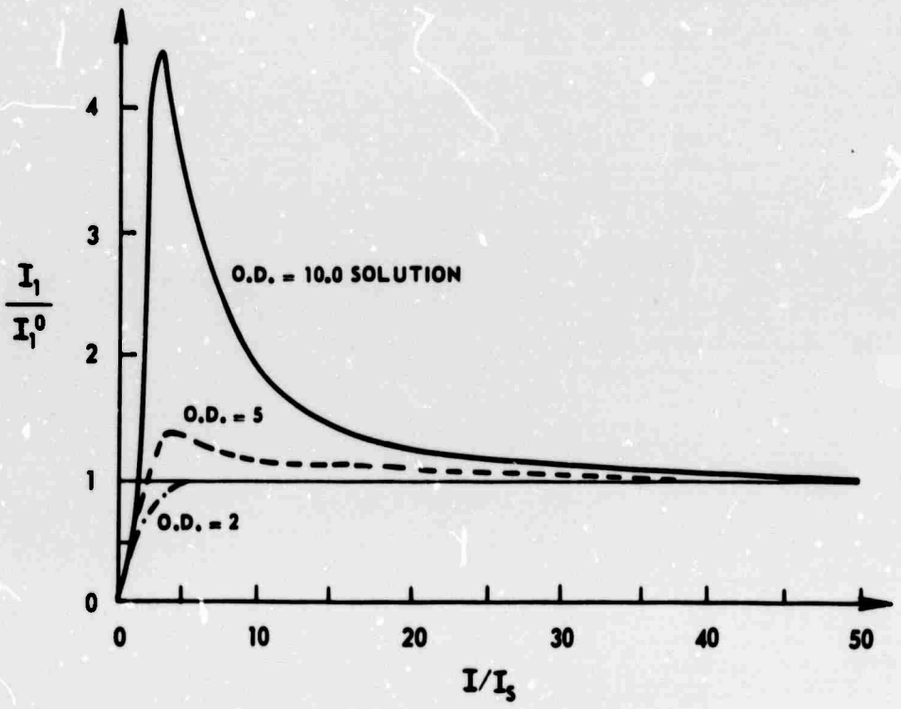

G920479-8

FIG. 12

VARIATION OF GAIN WITH PHASE MISMATCH

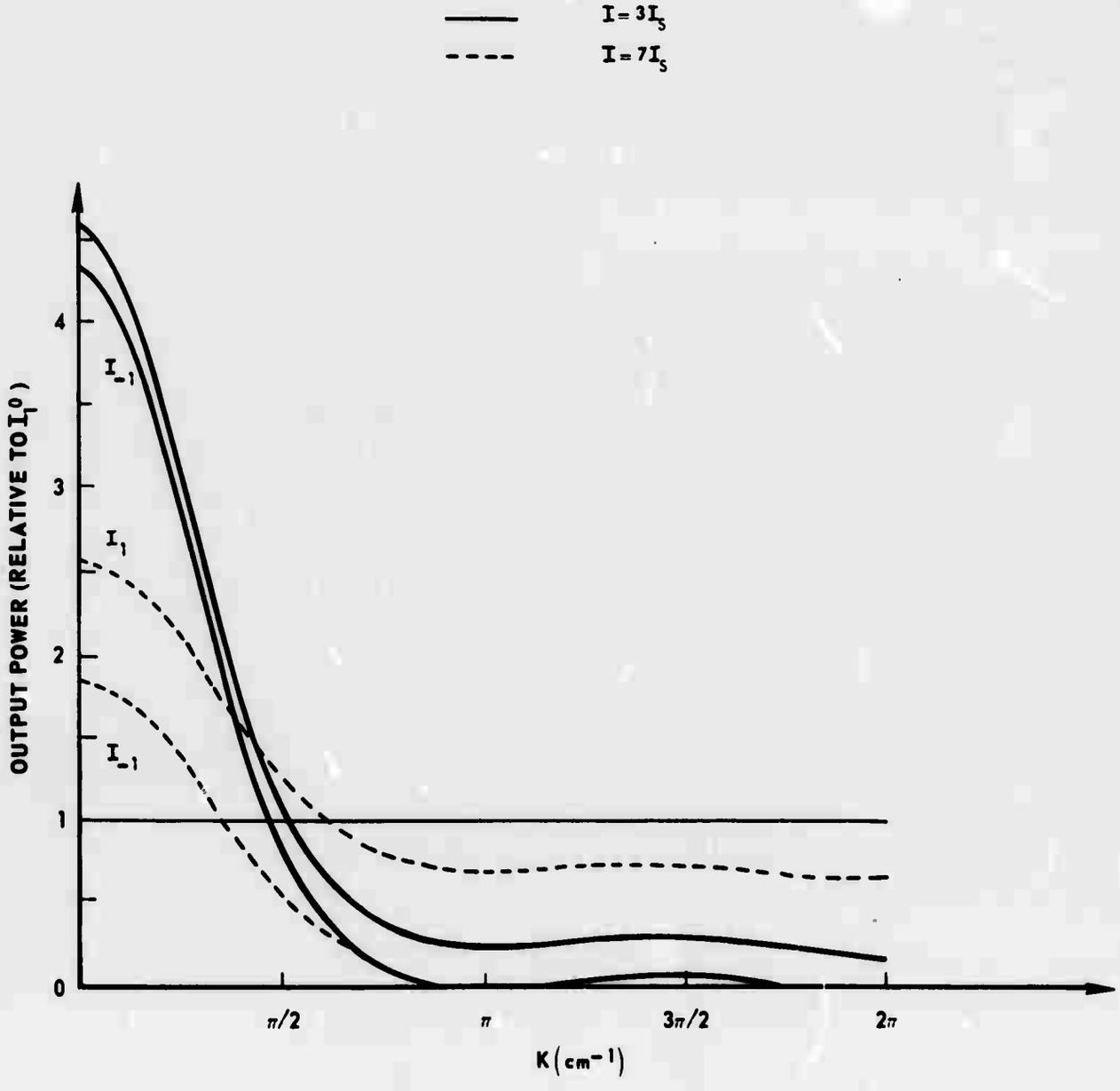

G920479-8

FIG. 13

SATURABLE ABSORBER TRANSMISSION CHARACTERISTICS

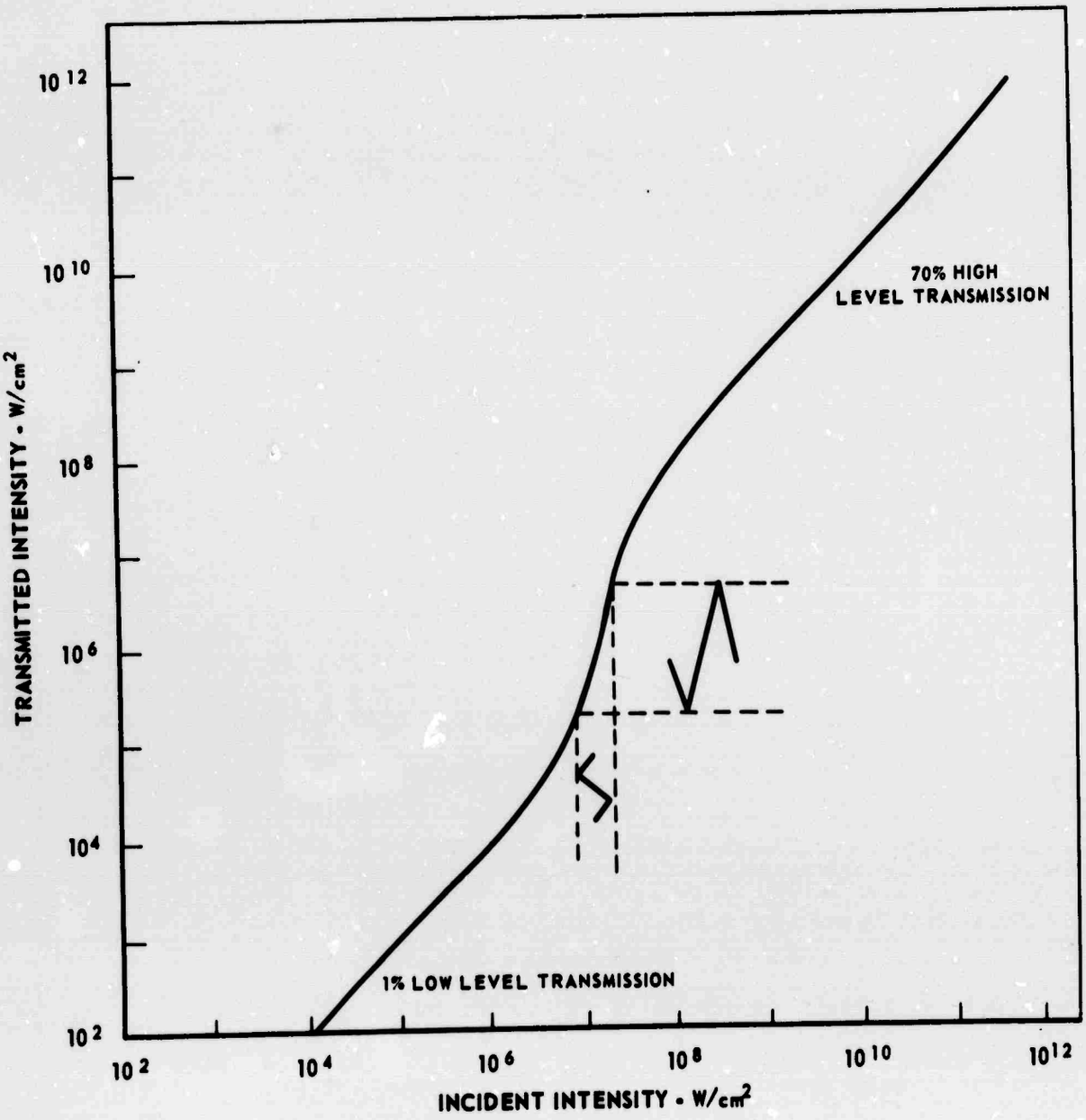

G920479-8

FIG. 14

GEOMETRICAL REPRESENTATION OF ADIABATIC INVERSION

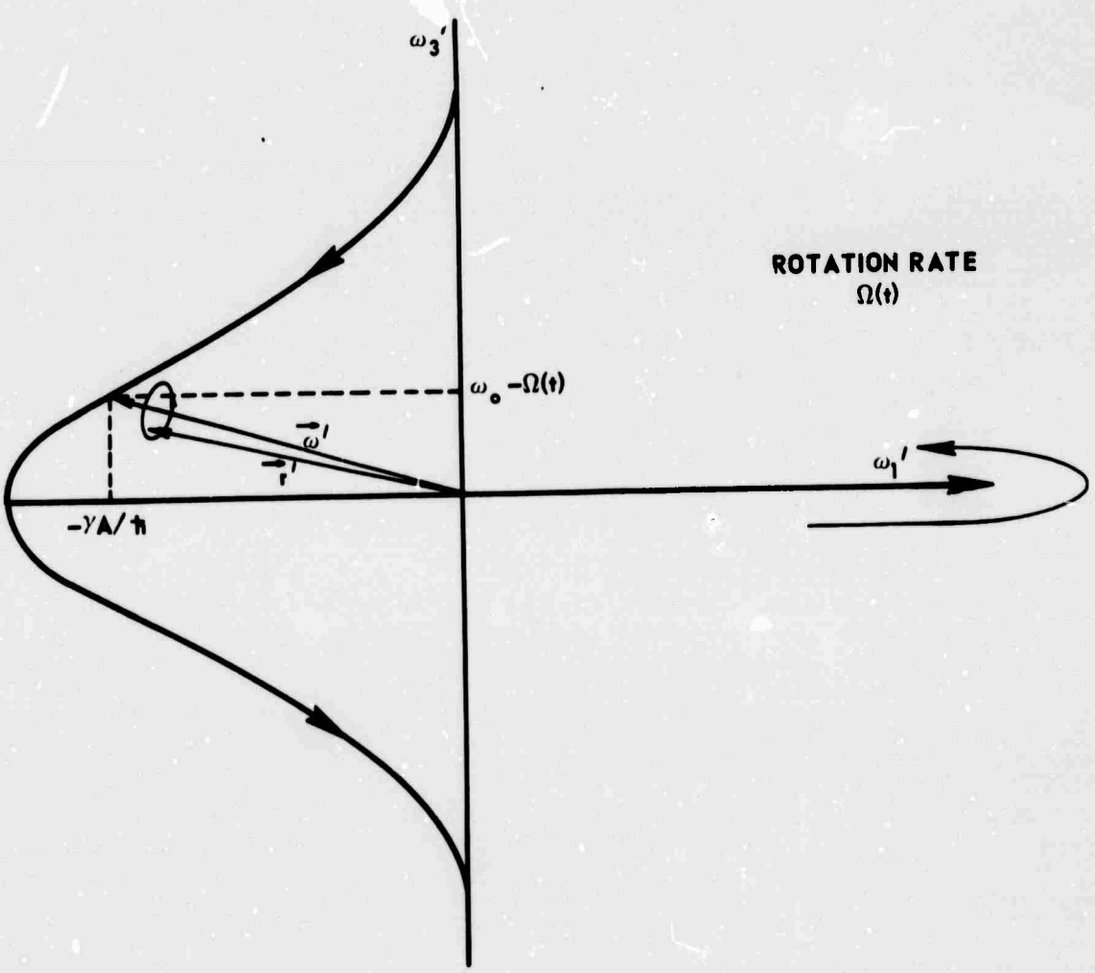

G920479-8

LASER CONFIGURATION FOR GENERATING FREQUENCY-SWEPT PULSES

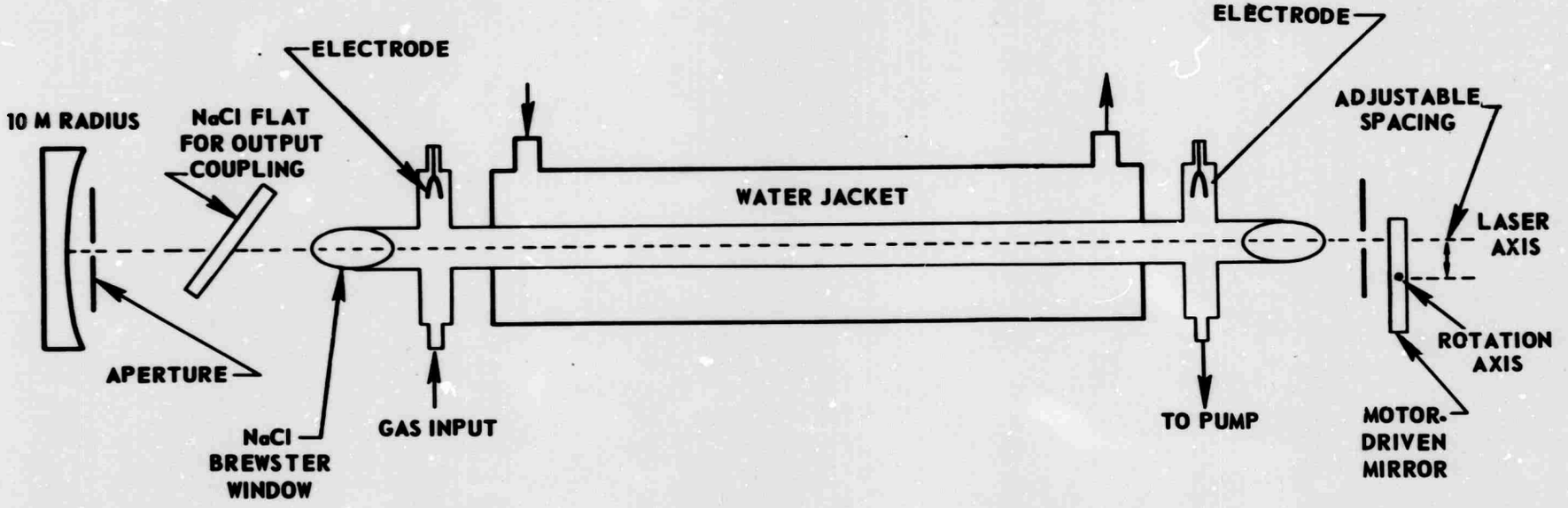

FIG. 15

G920479-8

FIG. 16

TYPICAL OSCILLOGRAMS OF CHIRPED Q-SWITCHED CO_2 PULSES

G920479-8

FIG. 17

EXPERIMENTAL EVIDENCE OF A CHIRPED Q-SWITCHED CO_2 LASER PULSE

(a)

(b)

G920479-8

FIG. 18

APPARATUS FOR PULSE COMPRESSION AND MEASUREMENT

G920479-8

ORIENTATION OF KDP CRYSTAL TO POLARIZATION OF REPETITIVE PULSE

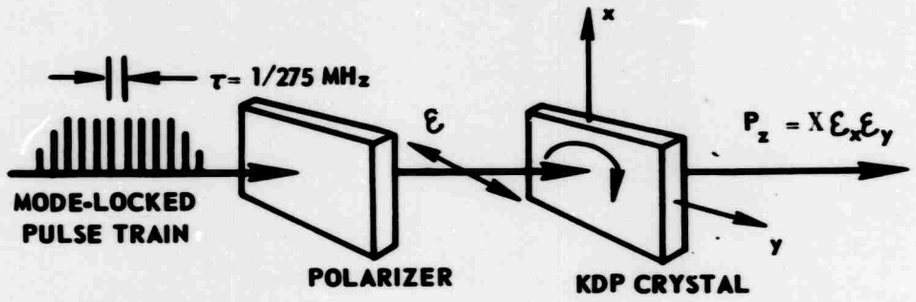

FIG. 19

G920479-8

OPTICAL RECTIFICATION SIGNALS AT 2.75 GHz
AS A FUNCTION OF CRYSTAL ORIENTATION

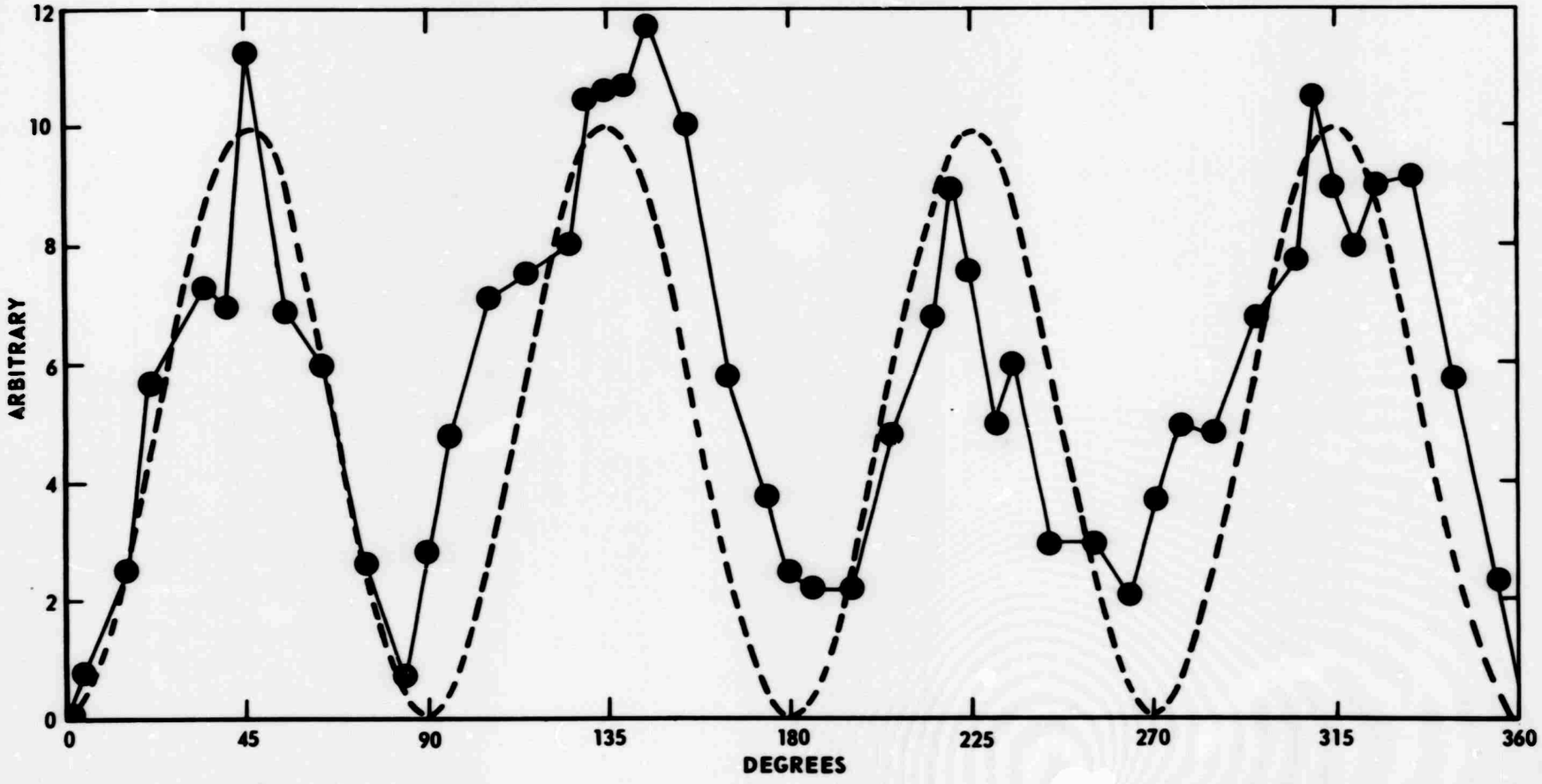

FIG. 20

G920479-8

FIG. 21

OPTICAL RECTIFICATION

RECEIVER OUTPUT

LASER OUTPUT

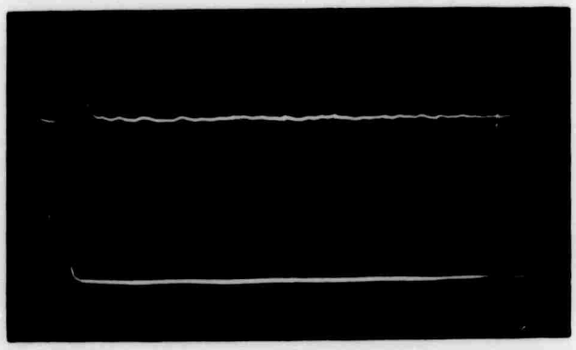

SWEEP SPEED:
0.5 μsec/div

6th HARMONIC - 850 MHz

LASER OUTPUT

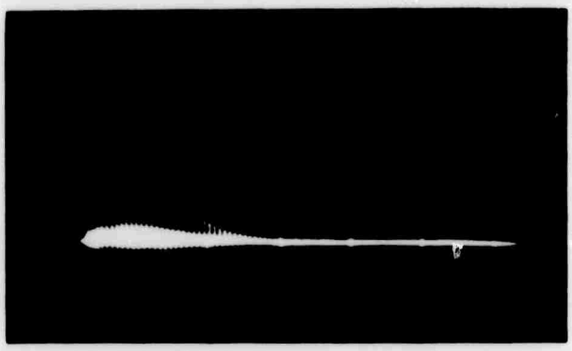

SWEEP SPEED:
100 nsec/div

G920479-8

EXPERIMENTAL ARRANGEMENT FOR MODE-LOCKED ORGANIC DYE LASER

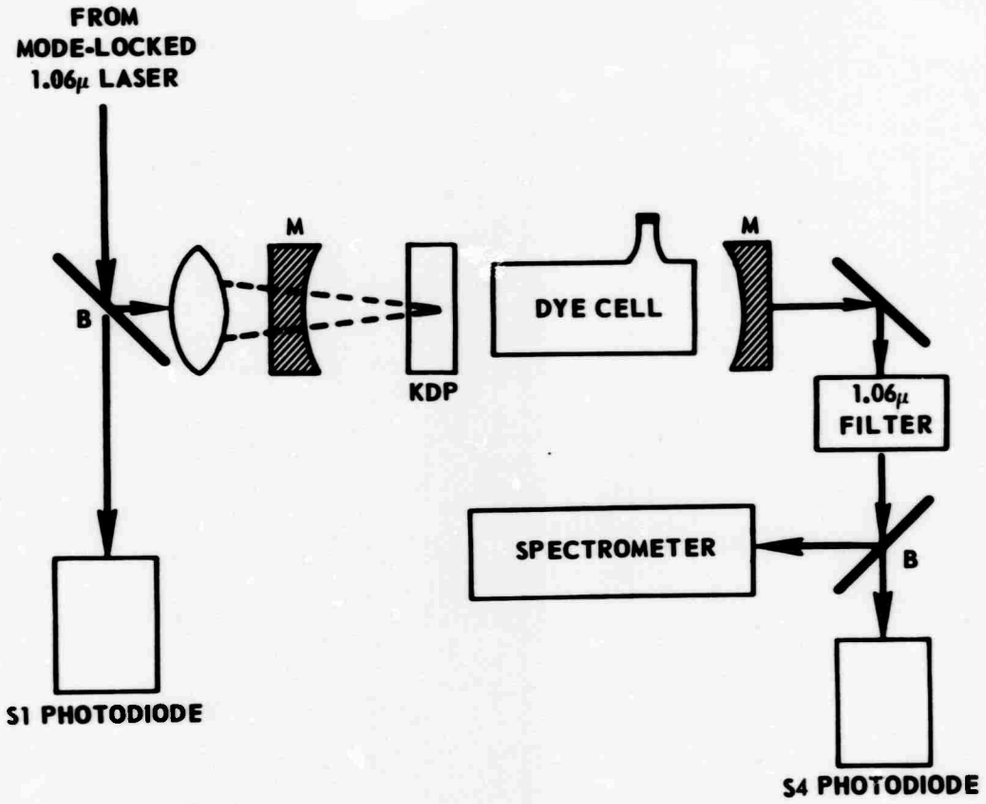

FIG. 22

G920479-8

FIG. 23

OSCILLOGRAMS AND SPECTRA OF A MODE-LOCKED DYE LASER

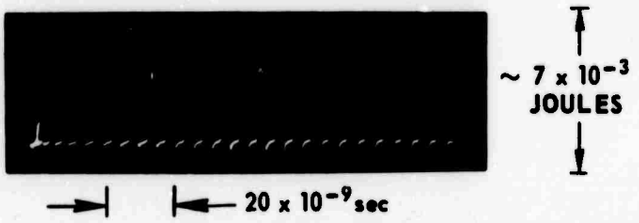

(a) PUMPING PULSE TRAIN INPUT

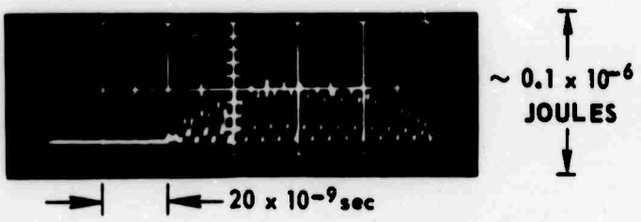

(b) DYE LASER OUTPUT

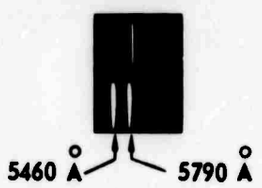

(c) SPECTRUM OF RHODAMINE B LASER

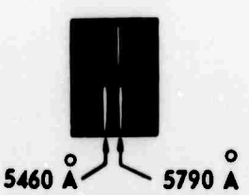

(d) SPECTRUM OF RHODAMINE 6G AND B MIXTURE

G920479-8

EFFECT OF CAVITY LENGTH VARIATION IN RHODAMINE 6G LASER

SWEEP SPEED 100 nsec/cm

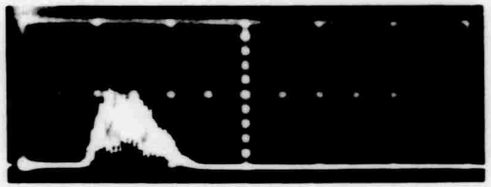

19 INCHES

18 INCHES

17.5 INCHES

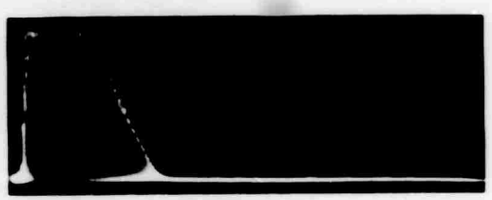

17 INCHES

FIG. 24

G920479-8

FIG. 25

MODE-LOCKED RHODAMINE 6G LASER PULSES AND SPECTRUM

17 INCH CAVITY LENGTH
SWEEP SPEED 50 nsec/cm

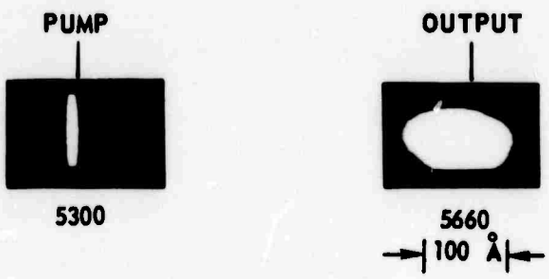

SPECTRUM OF OUTPUT PULSES

G920479-8

DYE LASER COAXIAL FLASHLAMP

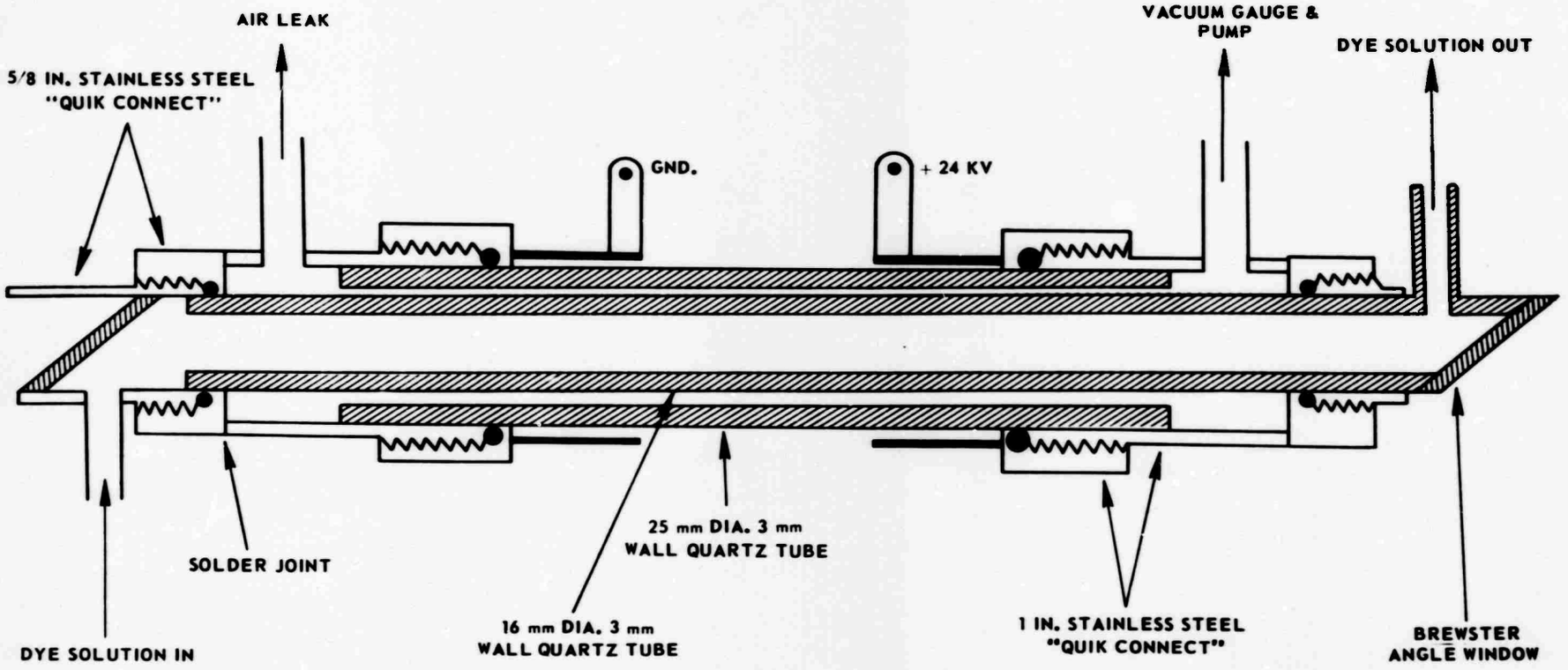

FIG. 26

Unclassified
Security Classification

DOCUMENT CONTROL DATA - R & D

(Security classification of title, body of abstract and indexing annotation must be entered when the overall report is classified)

1. ORIGINATING ACTIVITY *(Corporate author)*

United Aircraft Corporation
Research Laboratories
East Hartford, Connecticut 06108

2a. REPORT SECURITY CLASSIFICATION
Unclassified

2b. GROUP

3. REPORT TITLE

RESEARCH INVESTIGATION OF LASER LINE PROFILES

Scientific Annual Report for the Period 1 August 1967 to 31 July 1968

4. DESCRIPTIVE NOTES *(Type of report and inclusive dates)*

5. AUTHOR(S) *(First name, middle initial, last name)*

Anthony J. DeMaria, Michael J. Brienza, William H. Glenn, Jr., George L. Lamb, Jr., Michael E. Mack, and E. Brian Treacy

6. REPORT DATE	7a. TOTAL NO. OF PAGES	7b. NO. OF REFS
August 28, 1968	82	60

8a. CONTRACT OR GRANT NO.	9a. ORIGINATOR'S REPORT NUMBER(S)
N00014-66-C0344	G-920479-8
b. PROJECT NO. ARPA Order No. 306	
c.	9b. OTHER REPORT NO(S) *(Any other numbers that may be assigned this report)*
d. Project Cost Code No. 6E30K21	

10. DISTRIBUTION STATEMENT

Reproduction in whole or in part is permitted for any purpose of the United States Government.

11. SUPPLEMENTARY NOTES	12. SPONSORING MILITARY ACTIVITY
	Department of the Navy Office of Naval Research

13. ABSTRACT

This report covers work under Contract N00014-66-C0344 for the period 1 August 1967 to 31 July 1968. Topics discussed include theoretical and experimental work on the propagation of ultrashort pulses, measurement of nanosecond fluorescent decay times, light amplification in saturable absorbers, adiabatic inversion of quantum states, optical rectification and mode-locking of organic dye lasers.

DD FORM 1 NOV 65 1473

Unclassified
Security Classification

14. KEY WORDS	LINK A		LINK B		LINK C	
	ROLE	WT	ROLE	WT	ROLE	WT
Laser Line Profiles						
Picosecond Laser Pulses						
Ultrashort Pulse Propagation						
Fluorescent Decay Times						
Gain in Saturable Absorbers						
Adiabatic Rapid Passage						
Optical Rectification						
Organic Dye Lasers						
Mode-Locked Lasers						
Nonlinear Optics						